THE
AUSTRALIAN
NATIONAL
UNIVERSITY

RESEARCH SCHOOL OF PHYSICAL SCIENCES

ANU-P/452

BEAM FOIL SPECTROSCOPY

LECTURES BY S. BASHKIN

Notes by G.W. Carriveau,
Research School of Physical Sciences,
The Australian National University, Canberra

INSTITUTE OF ADVANCED STUDIES

ANU-P/452

BEAM-FOIL SPECTROSCOPY

LECTURES BY S. BASHKIN

(Notes by G. W. Carriveau)

This set of notes reports a series of four lectures given by Professor S. Bashkin, of the University of Arizona, Tucson, Arizona, in February and March of 1969.

These lectures were intended to give a general review of Beam-Foil Spectroscopy methods and applications.

Although Professor Bashkin looked over the notes before they went to print, any errors contained are certainly those of the reporter. The reporter must apologize for the poor quality of the figures contained; in most cases these were reproduced from slides. The reader is referred to the book Beam-Foil Spectroscopy, edited by S. Bashkin, where many of the original figures may be found, or to the references cited in most cases.

I am grateful to Professor Bashkin for the many hours he spent discussing the lecture notes. I would also like to thank Miss Norma Chin for her careful work in typing this manuscript.

G.W. CARRIVEAU

8th September, 1969.

Department of Nuclear Physics,
Research School of Physical Sciences,
The Australian National University,
CANBERRA ... A.C.T. 2600

BEAM FOIL SPECTROSCOPY

This lecture will concern work in two aspects of Atomic Physics, namely the structure of ionized atoms and the mean lives of excited electronic levels in atoms and ions.

The basis of the measurements described is the passage of a beam of energetic ions through a thin absorber [1]. The ions emerge from the absorber with some distribution of ionization states and, for each net charge, with some distribution of excited electronic levels. The decay of those levels is accompanied by the emission of radiation, the study of which is the heart of beam-foil spectroscopy.

A typical experimental arrangement [2] is shown in Fig. 1. The main difference from a similar experiment in Nuclear Physics is that the target is always the same: a thin foil. The particles pass through the foil and the light produced downstream from the foil is observed with an appropriate optical device.

A photograph of a target chamber and visible beam is shown in Fig. 2. The beam is invisible before reaching the foil. Light can be seen after transmission through the foil. This light can be studied using various methods of detection. It is possible to isolate certain charge states and spectral lines and obtain information about the decay of a particular level. The excited levels are produced in the foil and decay downstream. The intensity of the light decreases with the distance down-

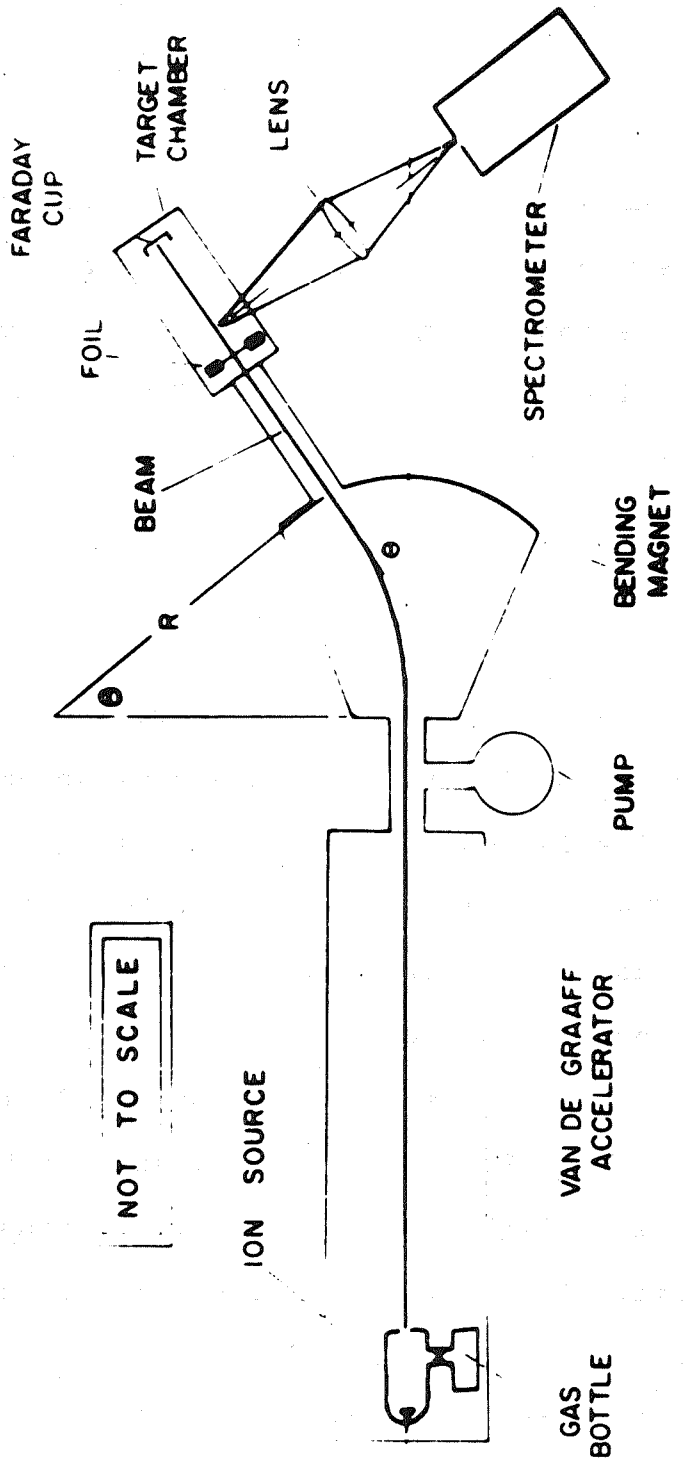

Fig. 1: Typical experimental arrangement.

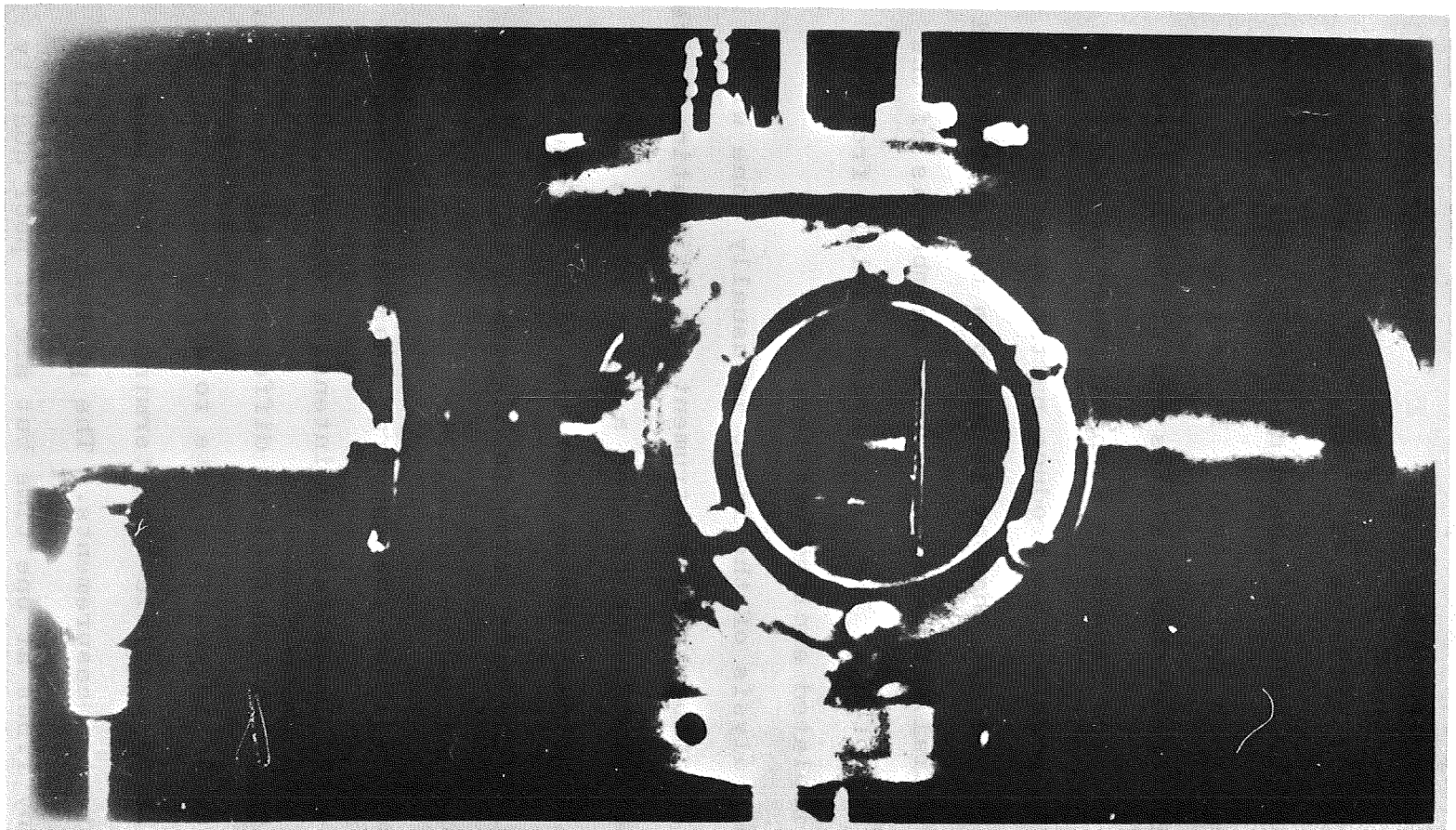

Fig. 2: Photograph of a beam of 2-MeV nitrogen after passage through a thin carbon foil. Beam travelling from right to left.

stream because of the finite mean lives of the excited levels. Since the particles travel with constant speed, there is a linear relationship between decay distance and decay time.

Figure 3 illustrates [3] the different charge states obtained by passing a beam of singly charged ^{16}O atoms through a thin carbon foil. It is possible to pick out ions of different charge states and study the light emitted from excited levels in each of those states.

It is possible to produce particles of high ionization. The target chamber is at room temperature and at ground potential. The vacuum in the chamber is of the order of 10^{-6} mm of Hg. The light arises solely from the decay of the isolated excited emitters.

The analysis of the light is usually done with some type of spectrographic instrument. A stigmatic device gives a 1:1 correspondence between a point in the source and a point at the detector so that the light at the slit and a picture of the slit taken in dispersed light is in faithful correspondence in intensity.

Figure 4 shows the spectral analysis of neon [4]. As can be seen the lines vary in intensity and in length. The differences in length reflect differences in lifetimes. The differences in intensity relate to differences in population. It is possible to determine the lifetimes of levels by distance measurements. The photographic plates shown give many lines at one time but are of poor quality for intensity measurements. It is possible to use photo-electric methods for intensity measurements. It is

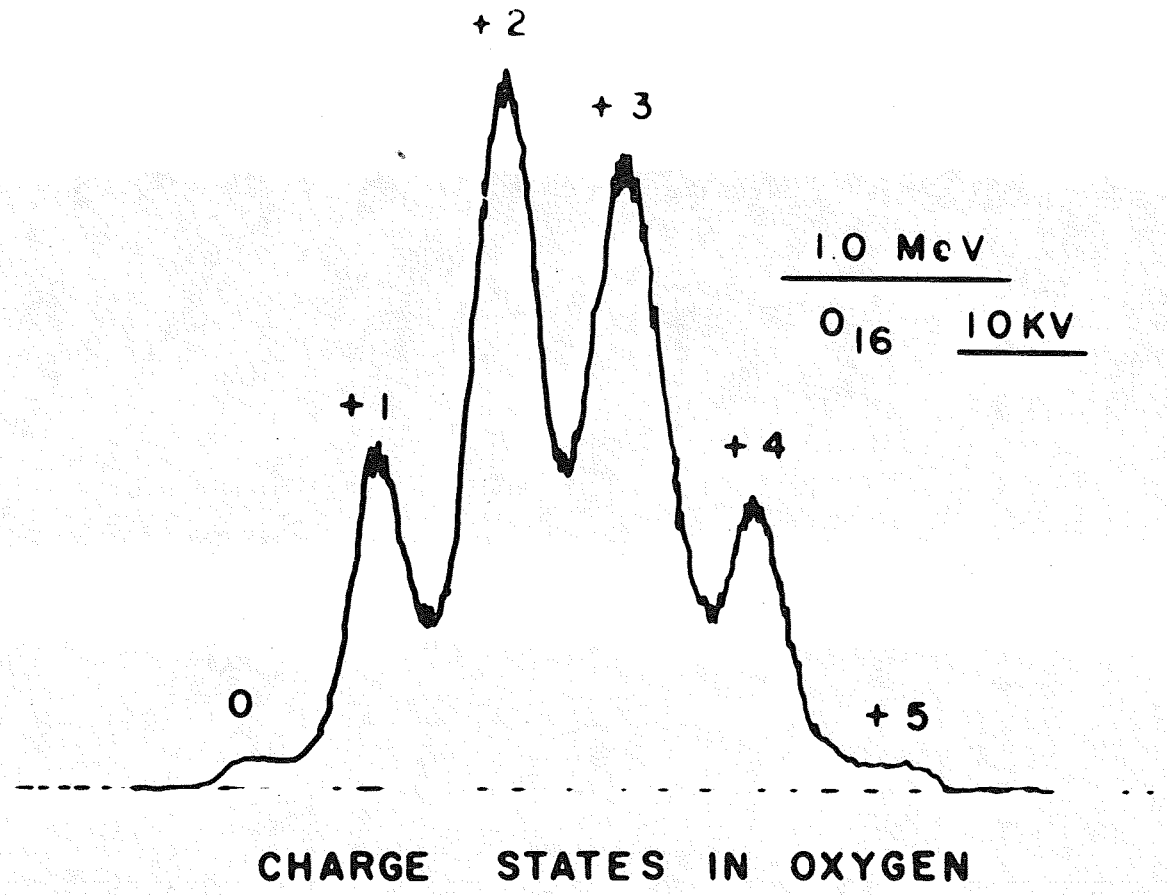

Fig. 3: Charge distribution of oxygen ions following transmission of 1 MeV O^+ ions through a thin carbon foil.

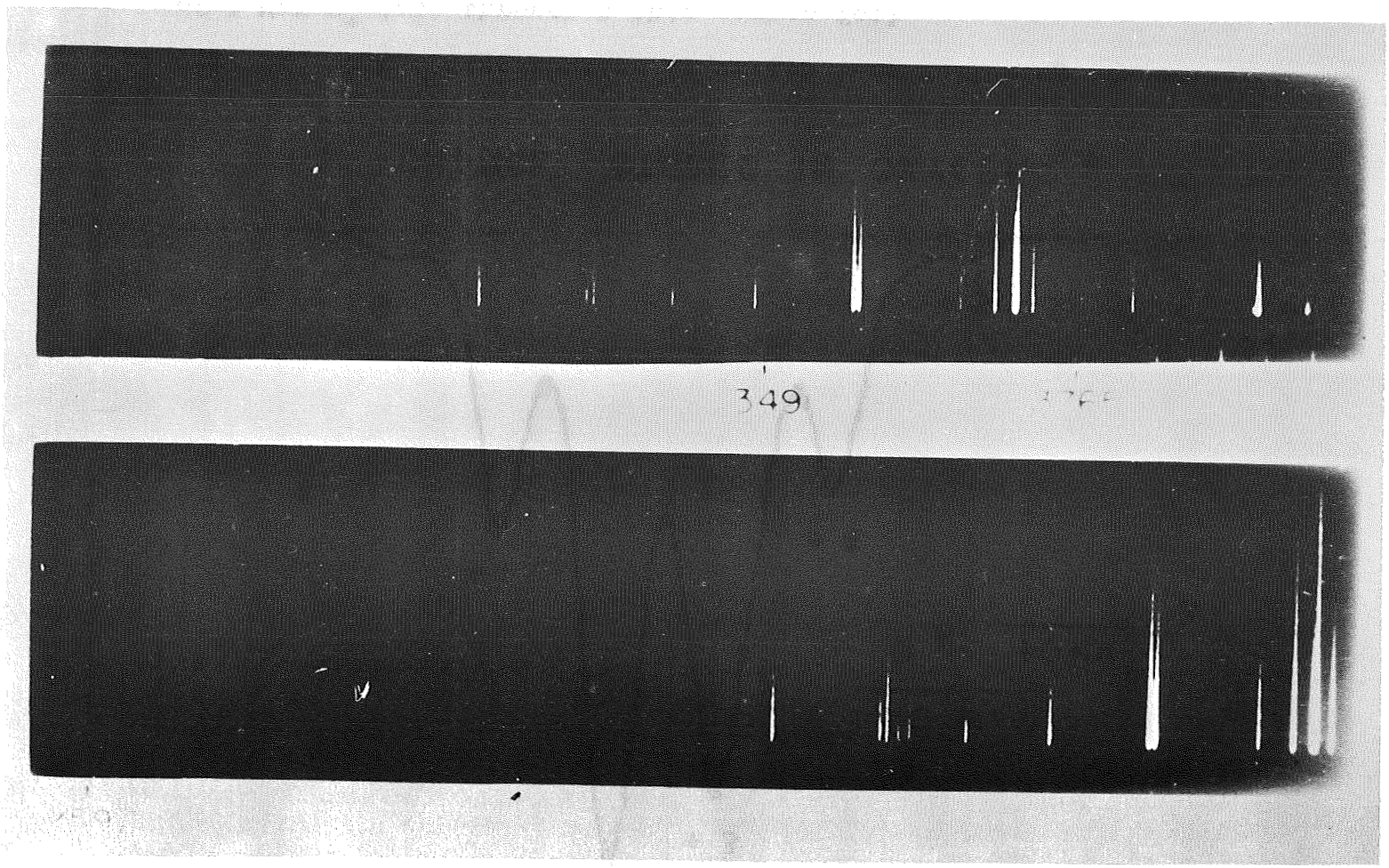

Fig. 4: Spectral analysis of neon. Incident energy 400 keV.

possible to get spectra from any element that can be accelerated.

A densitometer tracing of a nitrogen spectrum [5] is shown in Fig. 5. The lines labelled A, B and C are known multiplets of nitrogen ions (A and B) and possible contaminant lines from oxygen (C). It can be seen that it is possible to check wavelengths and intensities from tables. The lines are broadened by Doppler broadening, to be covered later. From Fig. 5 it can be seen that there are lines that do not correspond to decays from any known levels. These are strange lines and can be seen in every element studied except hydrogen and helium. In work done at the Carnegie Institution on sodium [6] over one hundred lines have been seen but only five identified. Measurements done at Cal Tech on iron [7] have shown that seventy-five per cent of two hundred lines seen are new. The novelty of such lines may be appreciated by remembering that spectroscopists use iron as a standard and have done so for a century.

In some cases these new strange lines may be the most numerous and intense of all. Figure 6 shows a densitometer tracing of a spectrum [8,9] from a beam of sulphur. It is possible to identify some lines but the most intense line at 3433 Å is not identified. Where do these lines come from? Is there an error or instrumental error? There are no known lines to within 50 Å of 3433 Å so there cannot be any instrumental error. The wavelength uncertainty in Fig. 6 is ±1 Å.

One advantage of the BFS system is that the

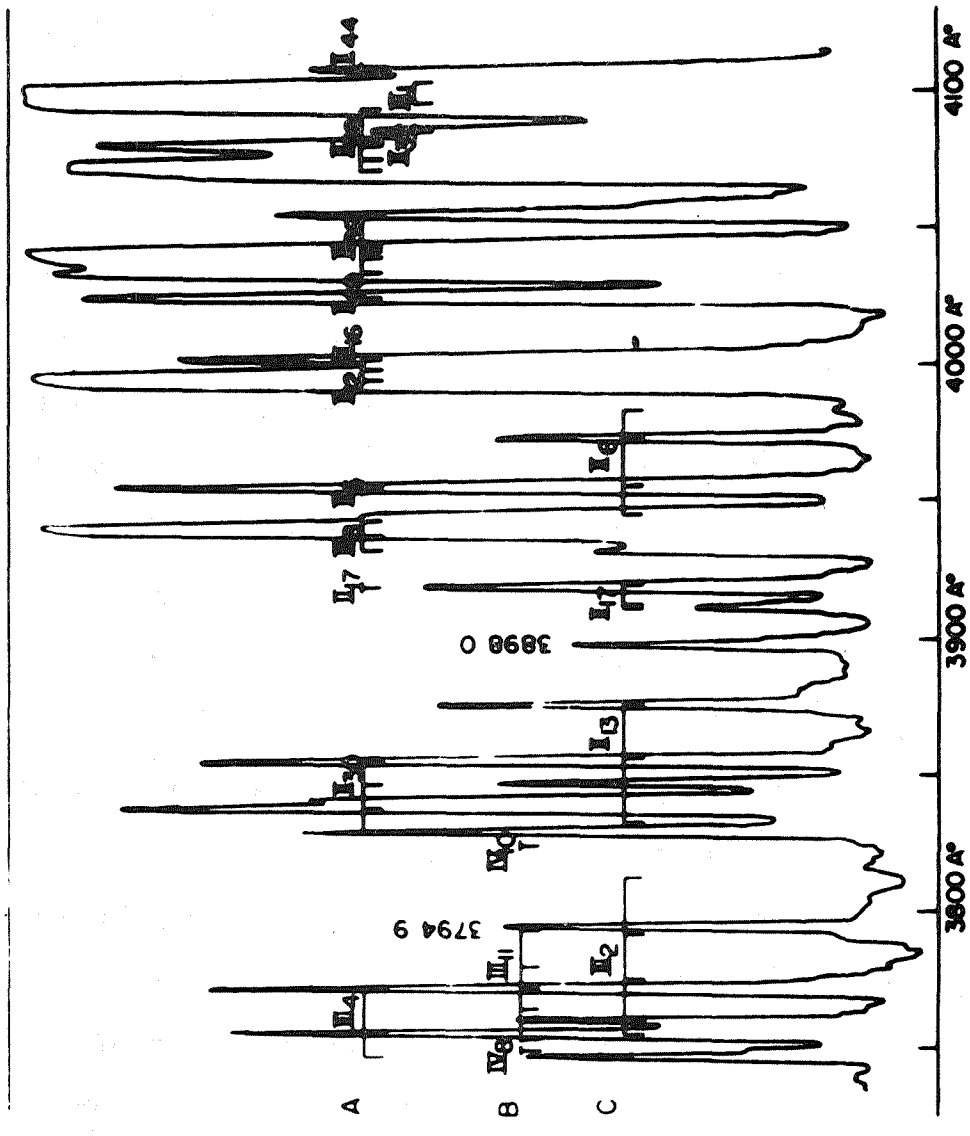

Fig. 5: Densitometer tracing of nitrogen spectrum. Incident beam 0.5 μamp of N_2^+ at 1 MeV. Exposure time 2 hours.

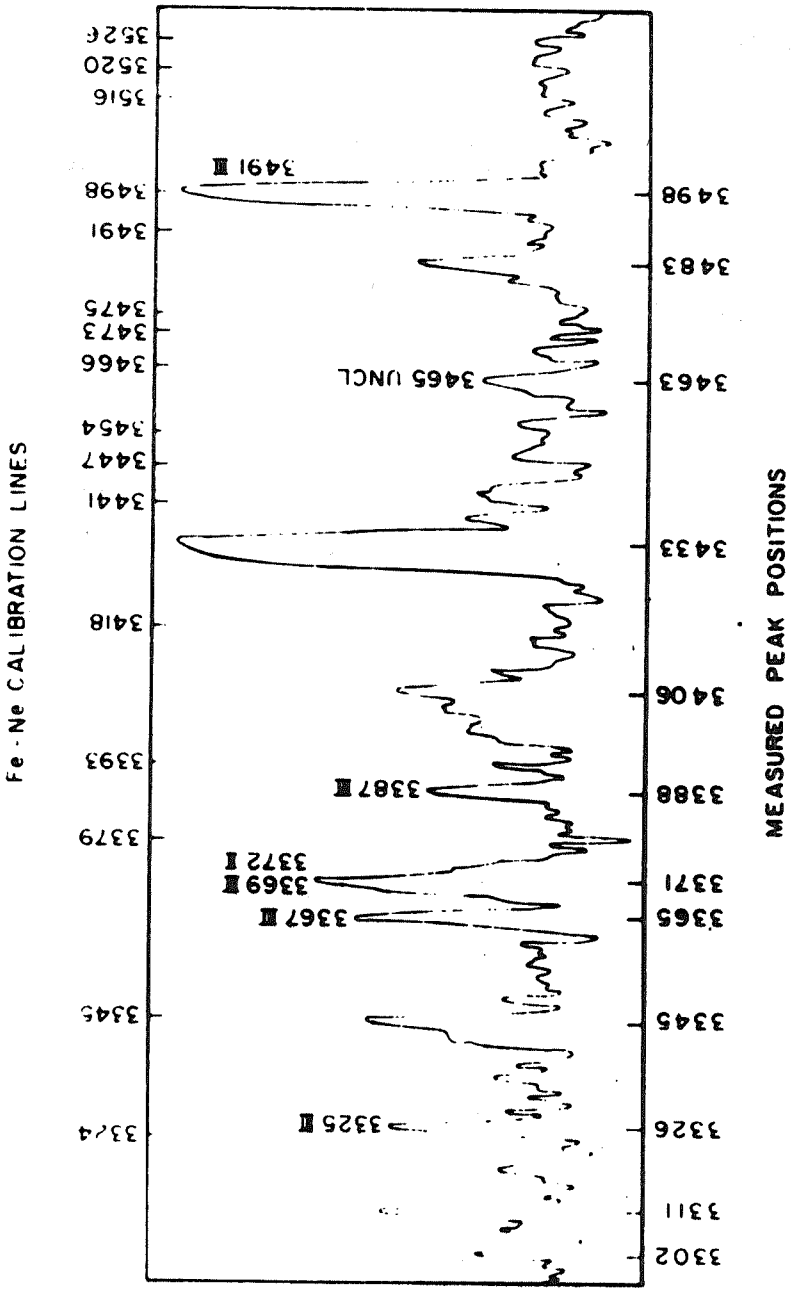

Fig. 6: Densitometer tracing of spectrum from beam of sulfur.

source is in a good vacuum. It is possible to get information on short wavelengths by direct coupling to a vacuum spectrograph. A spectrum of oxygen [10] in the range of 600 Å to 700 Å is shown in Fig. 7. It is possible to get to wavelengths of 100 Å. There are also unidentified lines in this wavelength range as in all ranges.

There are no known sources for these unidentified strange lines. There are no calculations to explain them. There is a need to reconcile these data with theory.

BFS is particularly valuable for lifetime measurements. In fact, BFS was used for the first lifetime measurements from multiply ionized emitters [11] and the first where the radiation is in the vacuum UV [11]. The results [12,13] of a mean life measurement of O V are shown in Fig. 8. It is possible to measure a dozen lifetimes in one day. O V has four electrons and so do many other ions. It is possible to look at the same structure in C III, N IV, etc., and compare the lifetimes with theory.

A study of oscillator strengths in the boron I sequence is shown [14,15] in Fig. 9. As can be seen, the theory and experimental data do not correspond. Measurements using the BFS method can show in detail to what extent the calculations are correct. Lifetime measurements are very sensitive to level wave functions.

While looking for mean lifetimes of certain levels, some complications may arise. Figure 10 shows decay curves from helium [16] that do not have the characteristic straight line corresponding to decay from one level. This indicates the presence of cascades. Any analysis of these

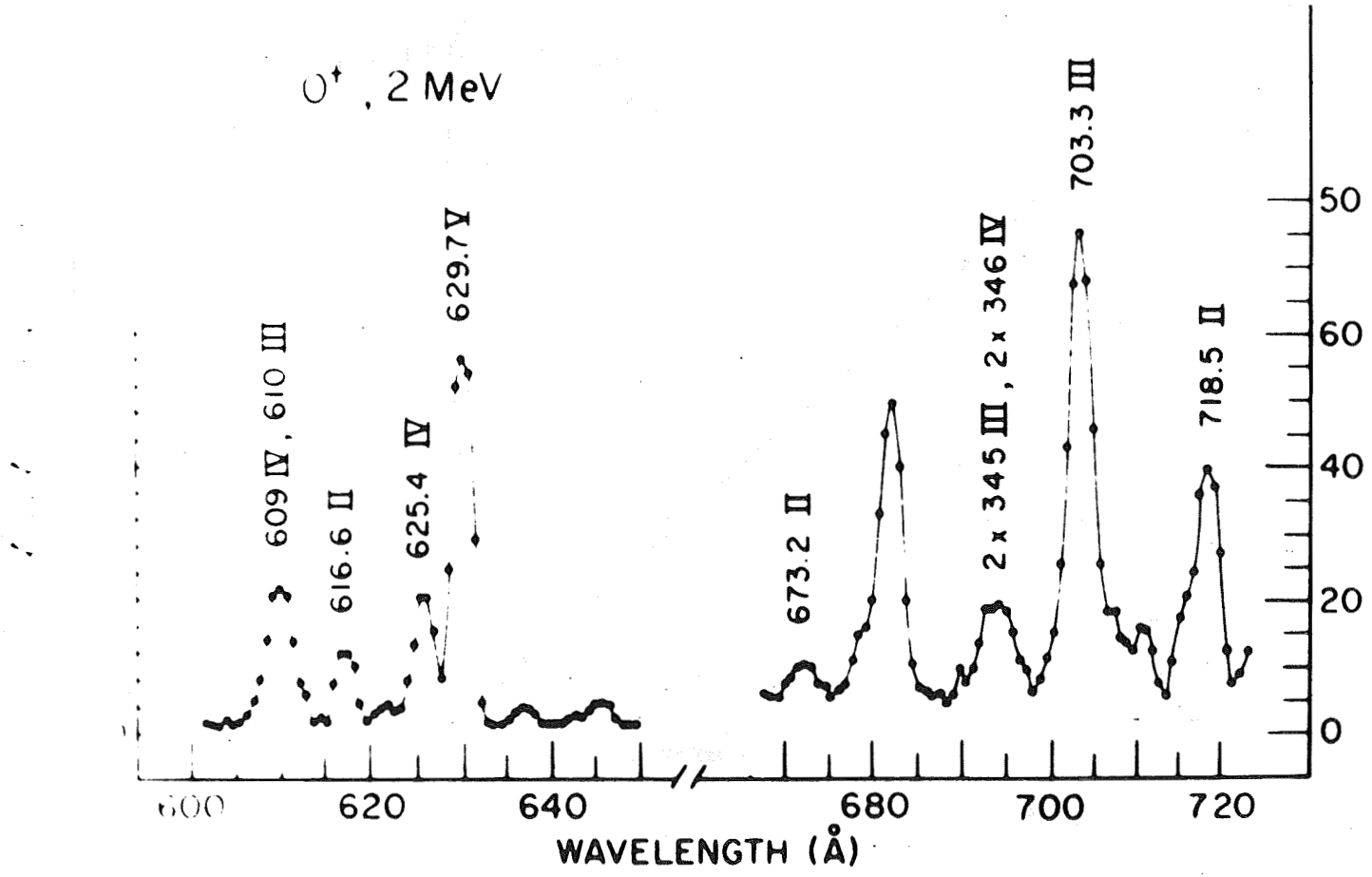

Fig. 7: The emission spectrum of multiply-ionized oxygen obtained with an incident 2-MeV O^+ beam and a 1000 Å-thick carbon foil. The line at 682 Å is unidentified.

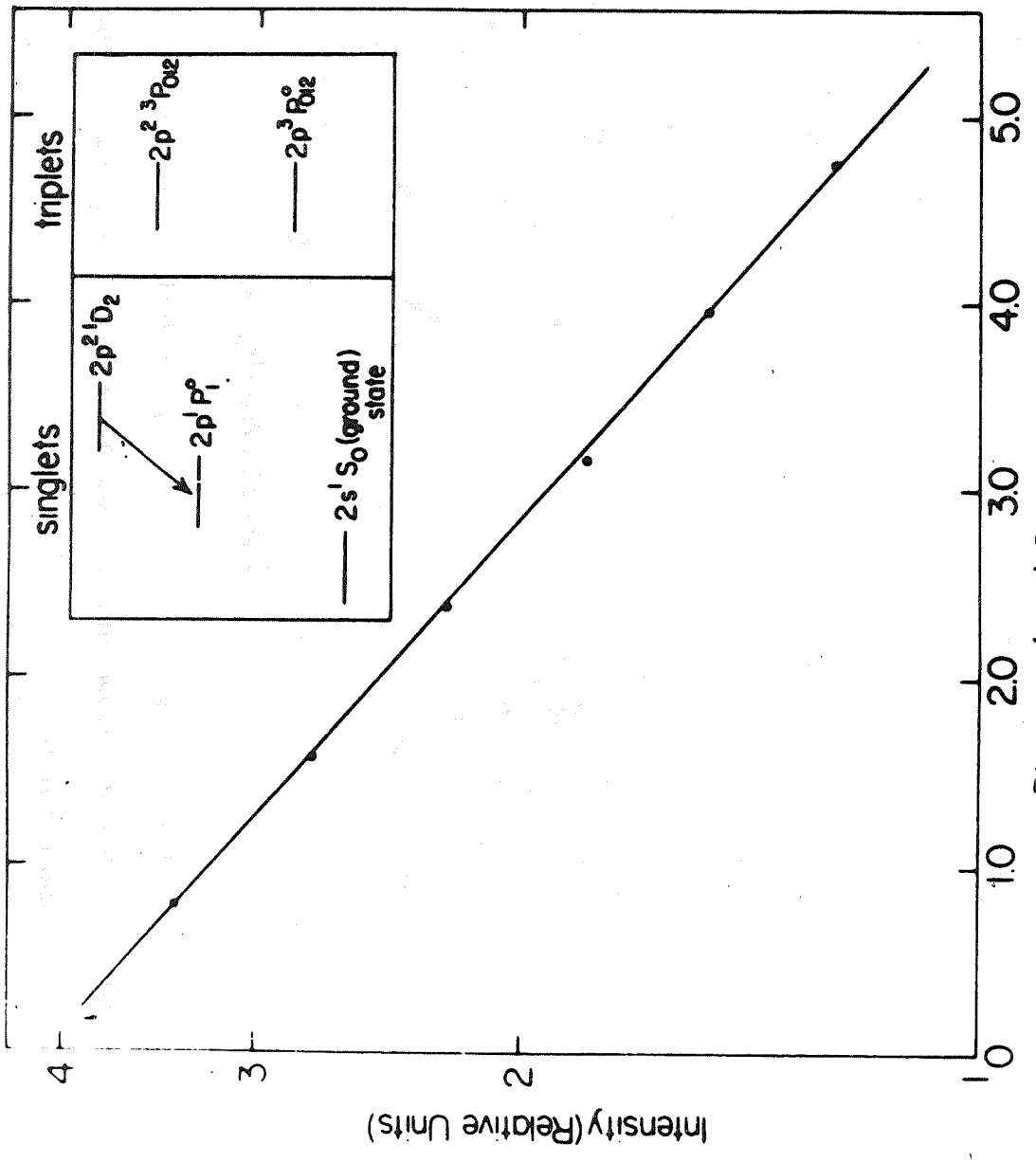

Fig. 8: Results of a mean life measurement of an excited level in O V using a photomultiplier.

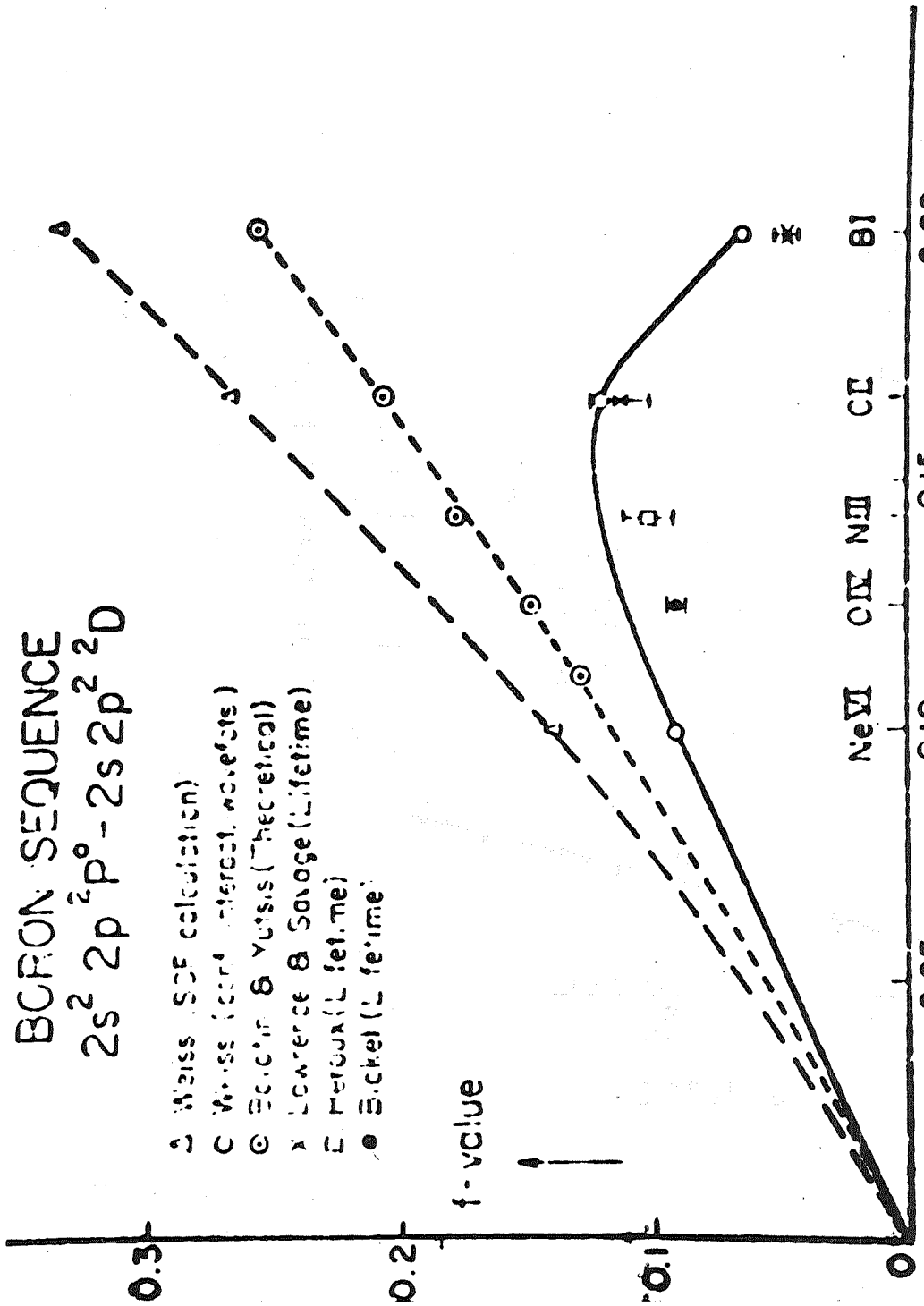

Fig. 9: f values vs. 1/z for the $2s^2\ 2p\ ^2P^o$ - $2s\ 2p^2\ ^2D$ transitions of the boron sequence.

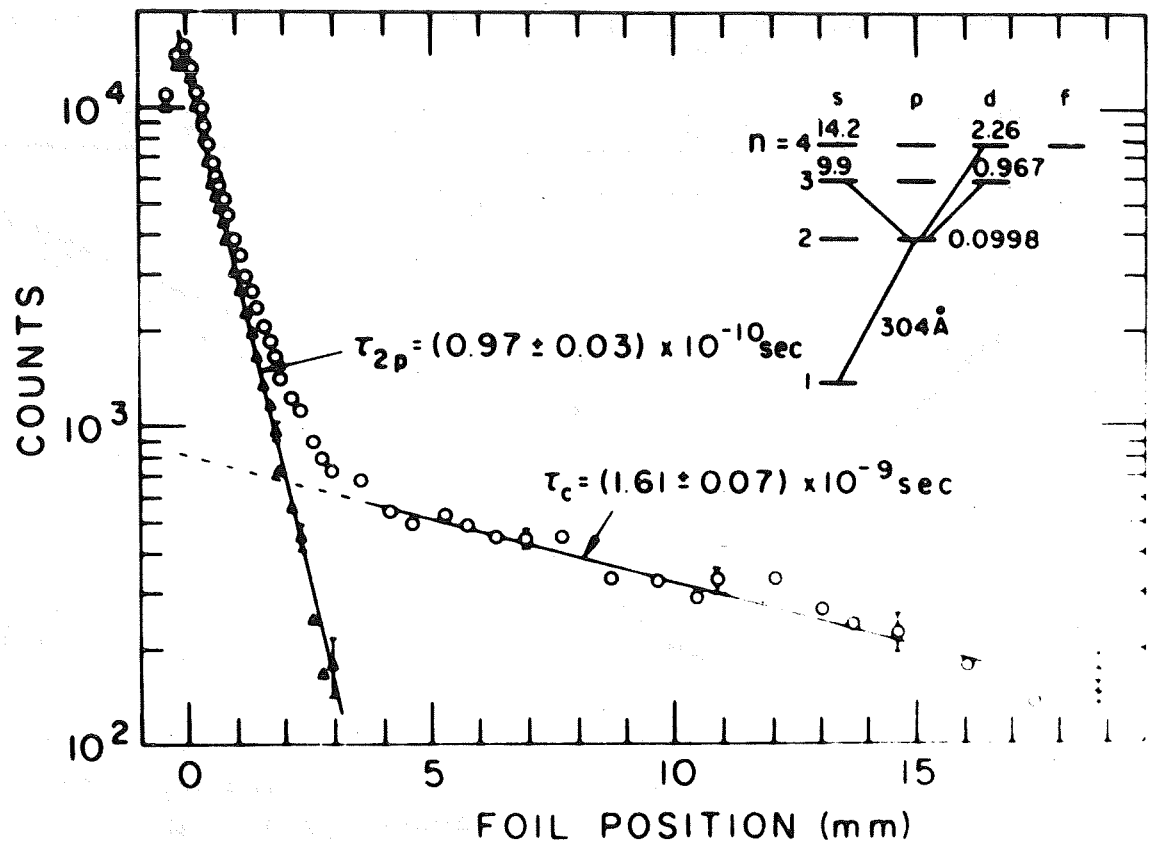

Fig. 10: Counts vs. foil position for the line He II 304 Å. The data were obtained with a foil thickness of 500 Å, a He^+ beam energy of 1 MeV, and a counting interval of 100 sec. O, data corrected for background noise; Δ, corrected for both noise and cascading. The calculated mean lifetimes in nsec of several levels in He II are indicated in the partial energy-level diagram.

data must include investigation of all contributions in this decay scheme.

It may be asked, 'Why look at lifetime data from hydrogen and helium? It is possible to make accurate calculations.' Condon and Shortley [17] give values accurate to one per cent. The point is that it is now possible to make measurements to check the accuracy and faithfulness of the theory.

Figure 3 illustrated various stages of ionization obtained in a foil excited beam. How is it possible to sort out different ionization states in the observation of emitted light? The traditional method of sorting out is difficult and cumbersome. As the nuclear charge increases, the nuclear force is different and the levels change. It is possible to determine ionization stages by following a pattern of spectral lines along an isoelectronic sequence but it is hard. There is an easier method that takes advantage of the beam-foil light source.

Figure 11 illustrates [18] the technique used to identify the various charge states. It is possible to apply a transverse electrical field to the beam and, as can be seen, the different charged states then follow different parabolic paths. An actual split beam [18] is shown in Fig. 12. This shows absolutely pure beams from two ionization states of nitrogen. When spectroscopy is done on the separated beams, there is no question of the state of ionization of the parent levels. In Fig. 12, it is also possible [19] to see different colours in the separate beams. This is a beautiful example of the effect of changing electron shielding.

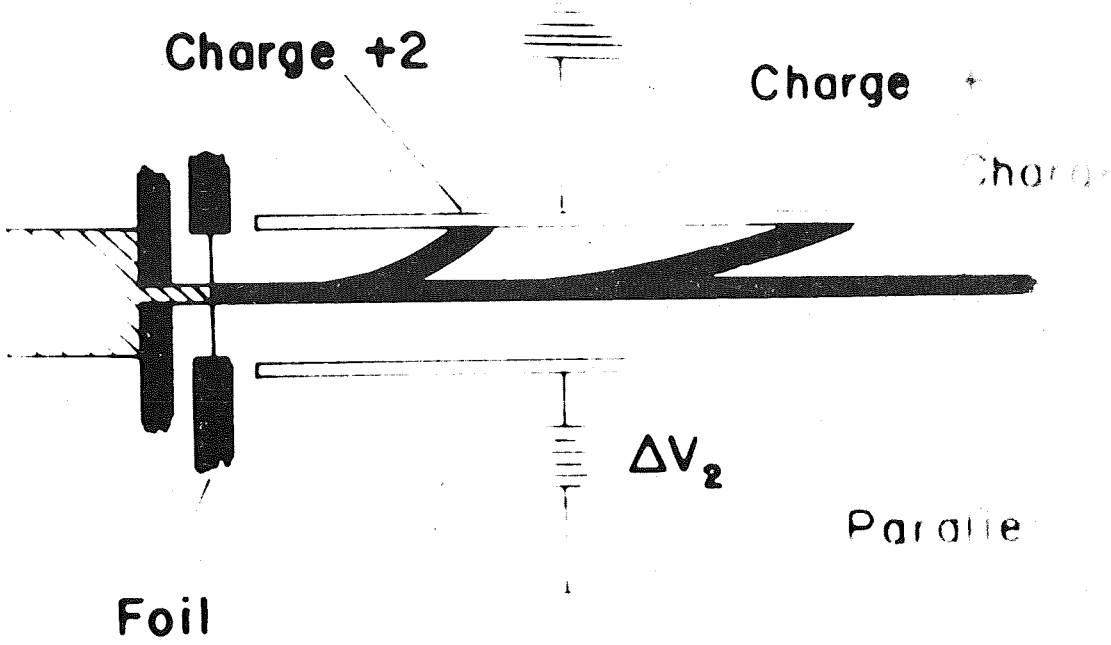

Fig. 11: Diagram of charge-splitting apparatus.

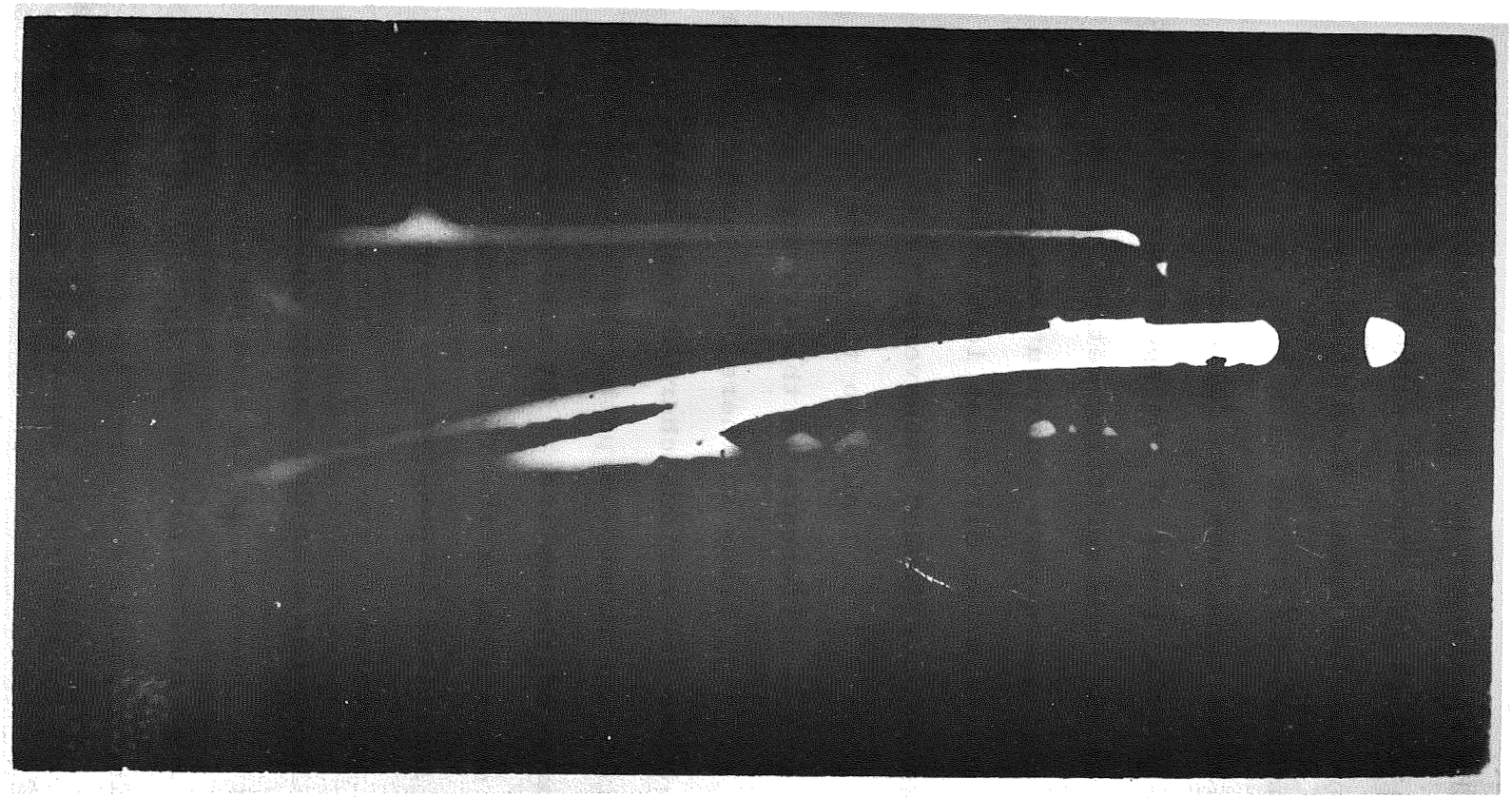

Fig. 12: Photograph of split nitrogen beams. The beam moves right to left. Incident particles N^+ at 2 MeV. Photograph taken by Malmberg, Bashkin, and Tilford at Naval Research Laboratory.

Some charge identification data [18] are shown in Fig. 13. This shows spectra taken using an applied electric field and moving the spectrograph. It is possible to identify the different charge states by their position on the plates. One unexpected result from this experiment is that at approximately 4540 Å, light with this particular wavelength was shown to come from two different stages of ionization. The resolving power of the spectrograph was not very good but, using the beam splitting method, it was possible to prove that there were contributions at a particular wavelength from two different ionization stages.

Past methods have looked transverse to the beams but it is also possible [20] to look into the plane of the split beams. There is a difference in the transfer of energy given to the moving beams so there is a change in the Doppler shift. Because the various charged components of the beam follow different parabolic paths the Doppler shift depends on the charge of the emitter. It also depends on the position seen downstream of the foil. Using the different Doppler shifts it is possible to determine different ionization states in the beam. Up to this time the only work published has been done using photographic plates as a detector. However, it is also possible [21,22] to bend a beam through slotted plates and look at the shift produced by applying a positive or negative potential. This displacement may be studied by observing the shift of a particular spectral line using a monochromator and a photomultiplier tube as a detector. With proper regard to optics this work can be done in the UV range.

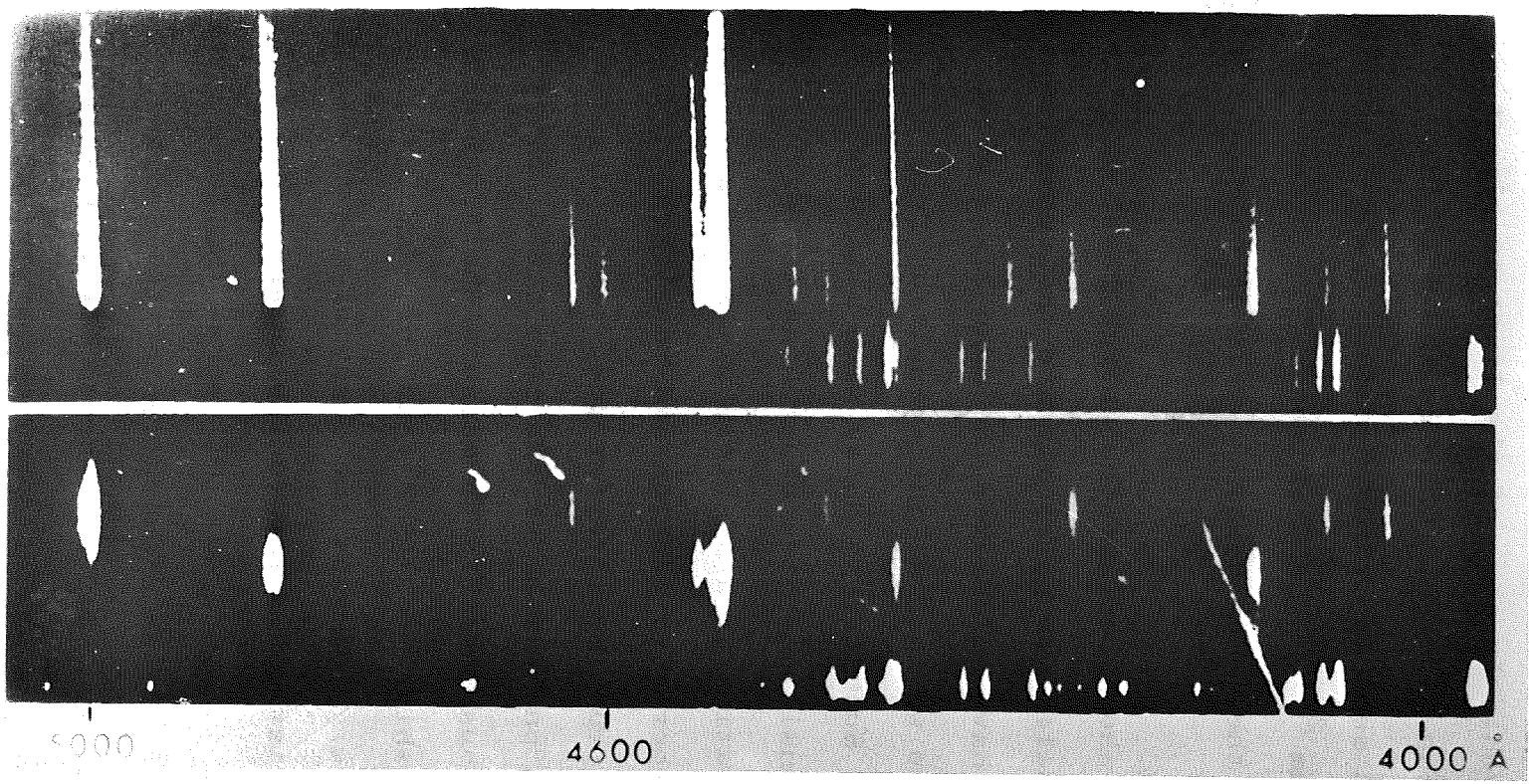

Fig. 13: Data obtained at Naval Research Laboratory (Ref. 18) on charge identification of source of spectral lines in nitrogen. The spectrograph scanned normal to the plane of the split beams.

When a beam of hydrogen or single-ionized helium is passed through a small transverse field a different effect may be observed. In some of the lines an almost periodic variation can be seen. This is shown in Fig. 14. The effect was first seen in hydrogen data [23] and later in singly-ionized helium [24,25], and arises [26,27] because of the Stark effect on the ℓ-degenerate levels of one-electron systems.

Figure 15 shows part of the energy level diagram for hydrogen. The selection rules dictate the transitions. Condon and Shortley have calculated the mean lives of the transitions. Suppose we look at the transition from the $n = 6$, $\ell = 0$ level. Such levels decay with a life of 570 nsec. Other transitions give other mean lives.

The application of a DC field mixes the adjacent ℓ-levels in a quasi-periodic fashion and to alternate with constructive and destructive interference. A calculation can be made using as one parameter the zero field energy difference. It is thus possible to measure the frequency and obtain the Lamb shift in high Z ions for high ℓ values.

In high energy physics the decay of the K^o meson shows some characteristic similar to the interference effects we have seen in hydrogen. Of course the force field is entirely different but an examination of the Stark-modulated spectrum of hydrogen reinforces the view that the K^o is composed of two systems of opposite parity and different lifetimes and that the two systems can interfere with one another.

As in any type of measurements there are some

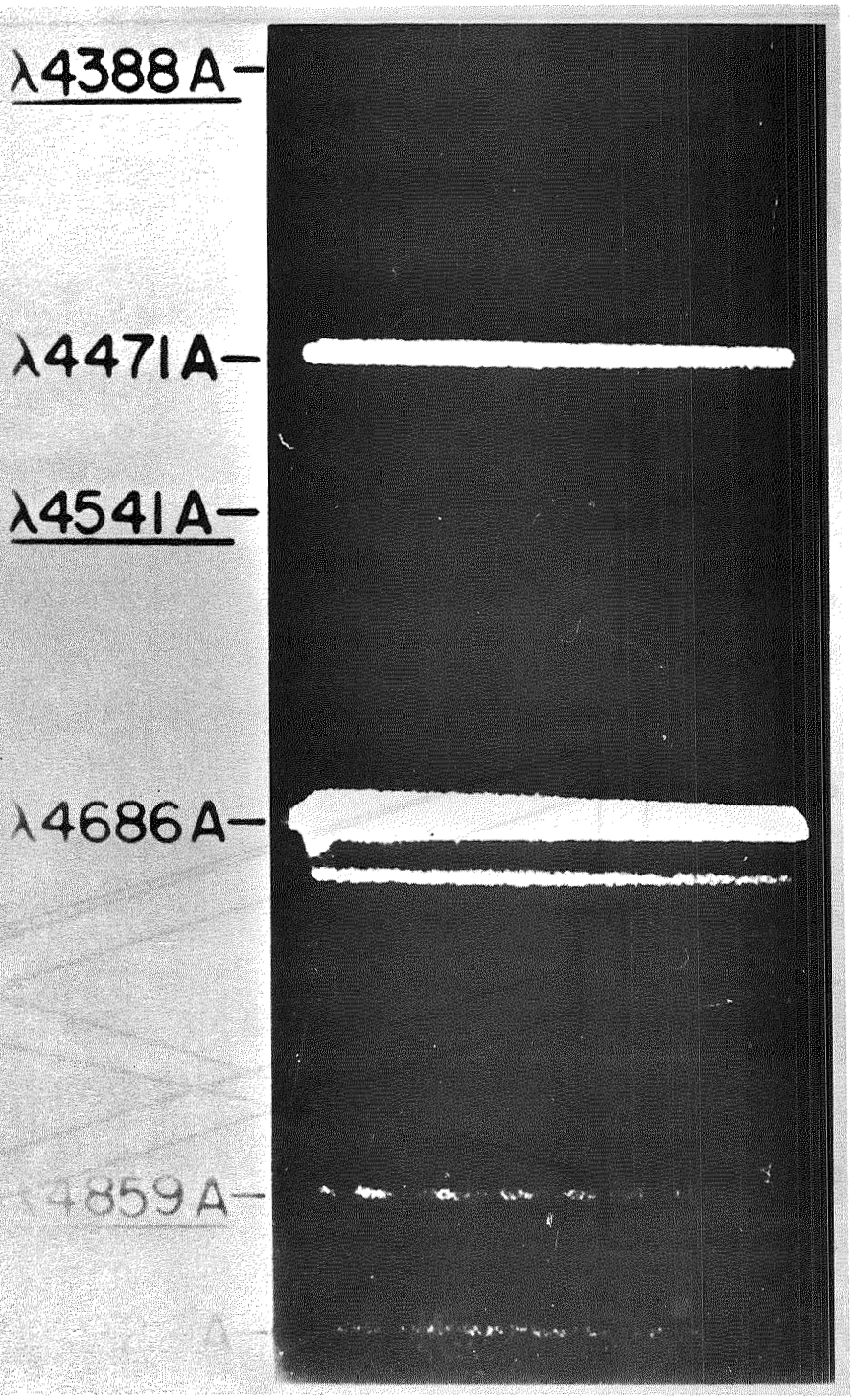

Fig. 14: A partial spectrogram showing several spectral lines in He I and He II.

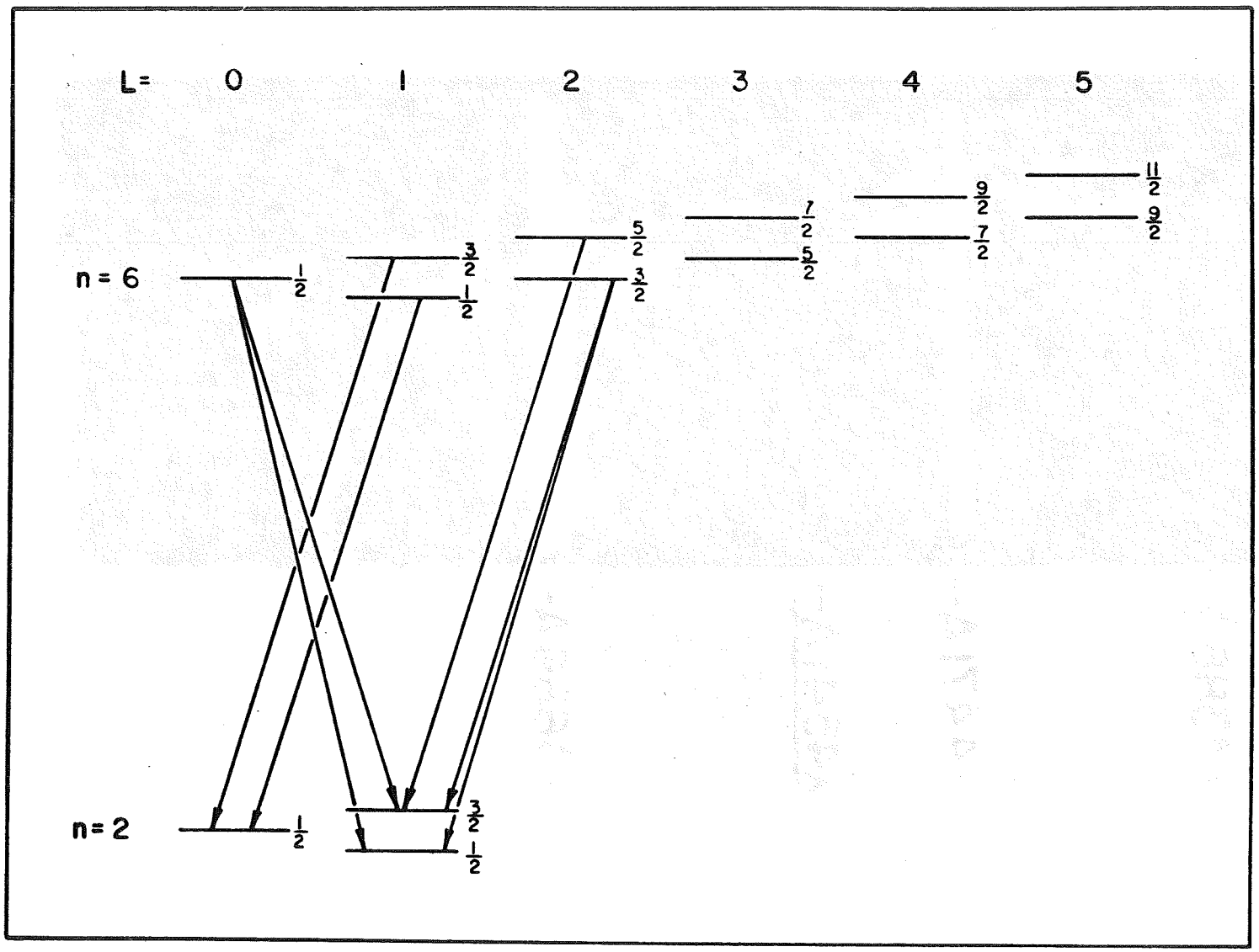

Fig. 15: Part of energy-level diagram for hydrogen. Not to scale. The transitions shown by the arrows comprise the 'line' Hg.

inherent handicaps involved. A major problem in interpreting the wavelength data is that the spectral lines are severely broadened by the Doppler effect. Figure 16 illustrates the source of this problem. The wavelength change depends on where the light from the beam enters the lens and also on the speed of the emitting particles. As can be seen there is a red-ward shift and broadening proportional to the distance downstream from the foil. The wavelength shift may be up to 10 Å in some cases. There is however one possible way to reduce the Doppler broadening (but not the Doppler shift).

Figure 17 shows a schematic diagram [28,29] of the axicon system to be used to reduce Doppler broadening. The principle of the system is that photons of the proper wavelength enter the reflector at 90^{o} and are then focussed at the proper place on the entrance slit of the spectrograph. Photons at other angles are focussed at some other point. This system uses focal isolation to reduce the problem to the 90^{o} Doppler shift. The broadening seen is determined by the width of the spectrometer aperture used (by the angular range accepted). With the use of this system there is no reduction in the speed of the optics, for only useless light is thrown out.

If it is possible to get good sharp line shapes it will be possible to do other types of experiments. In nuclear physics it will be possible to do charge distribution studies. With conventional methods there are problems making corrections for electron shielding. Using beam-foil spectroscopy methods it is possible to get rid of most of the electrons which cause the shielding.

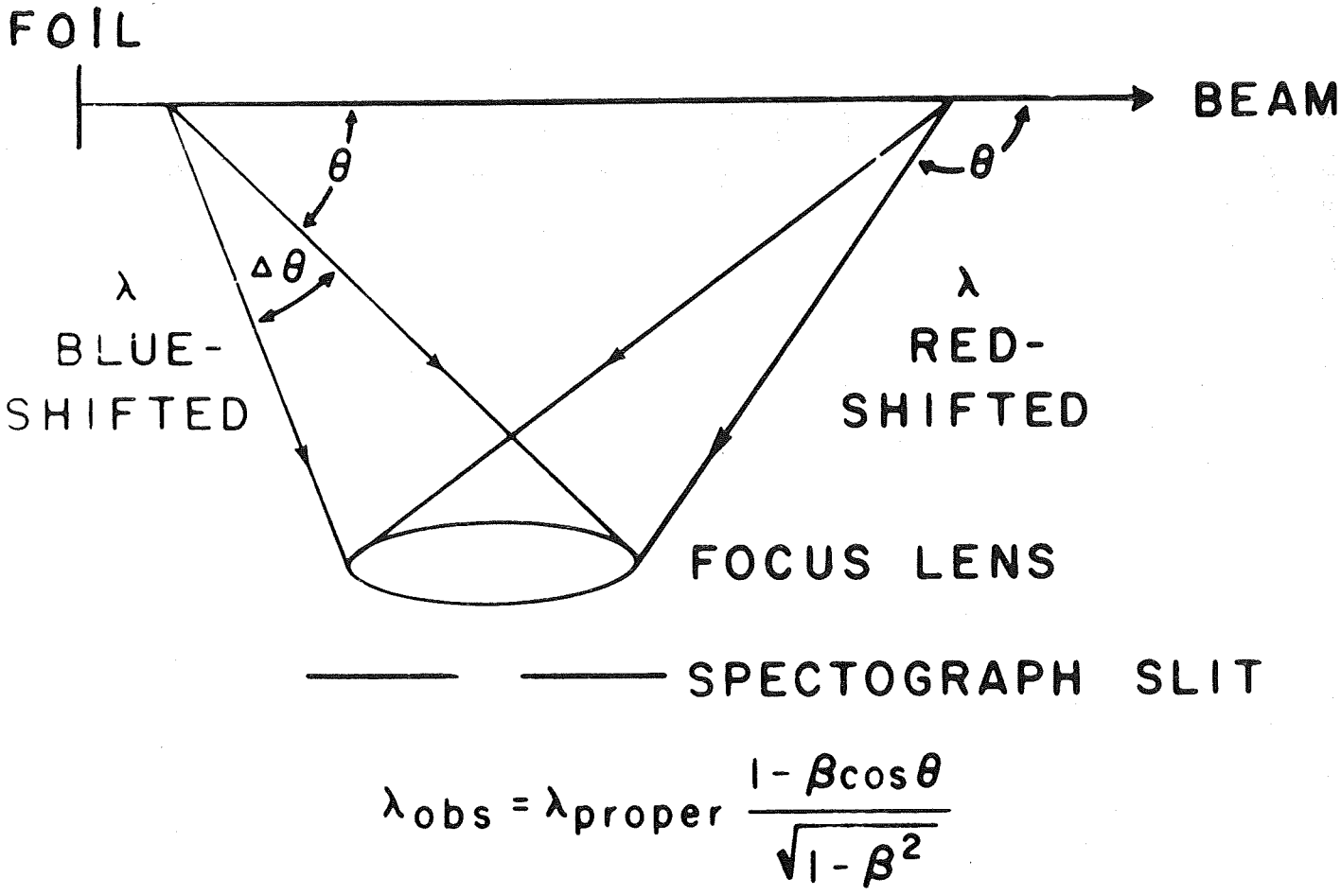

Fig. 16: Doppler broadening due to speed of emitters and finite acceptance angle of spectrograph.

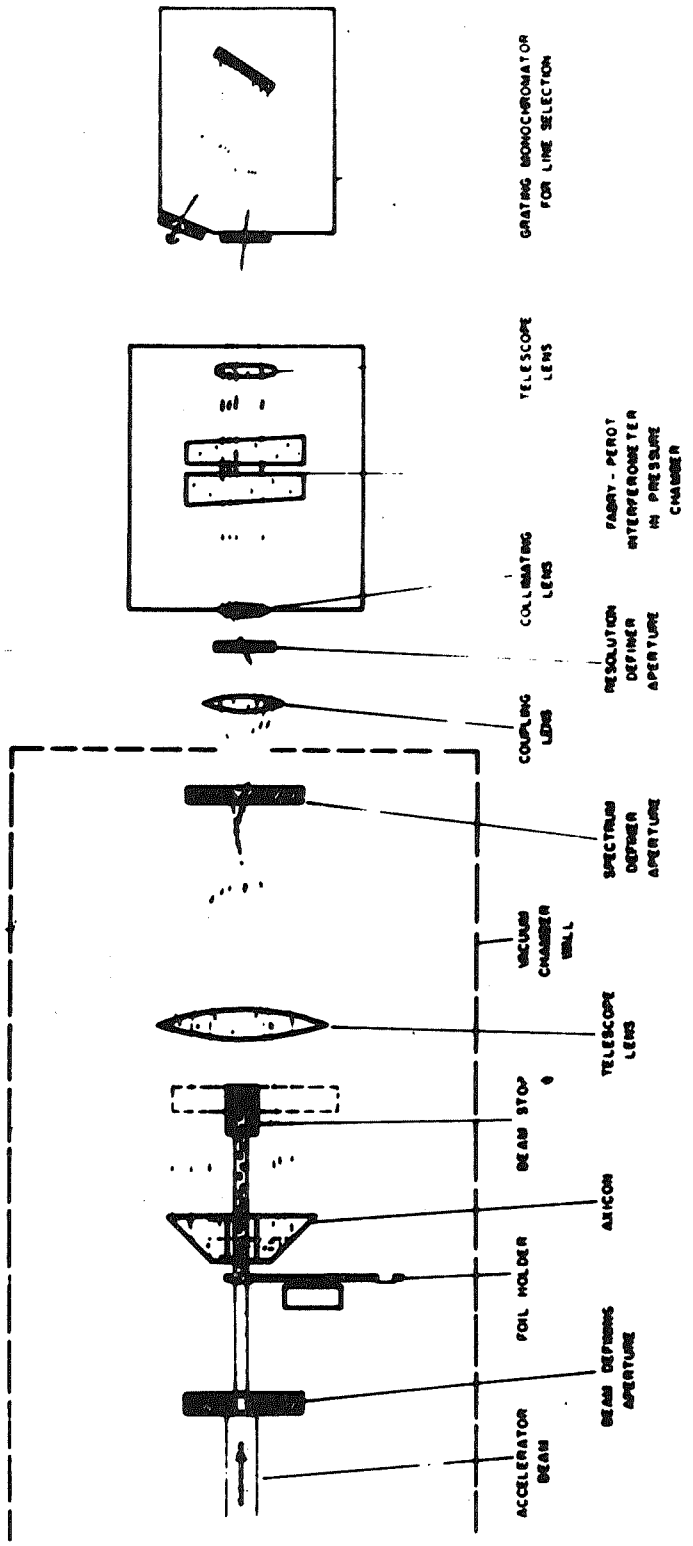

Fig. 17: Axicon system to reduce Doppler broadening.

WAVELENGTH MEASUREMENTS

The basic information in the spectroscopic measurements is contained in the intensity - wavelength distribution. The problem is to get good information from this distribution. One aspect of the wavelength determination is related to the relative intensities seen in the distribution. One must look closely for peaks in the spectra and there may be a problem in the signal to noise ratio. There may be problems inherent in the type of detecting system used. Photographic plates may give problems through graininess of the emulsion, or from background light, or from reciprocity failure, especially in long runs. A photomultiplier tube has a dark current that can be reduced by cooling. It may be possible to subtract the residual signals from the data.

The problem of Doppler broadening was discussed earlier and illustrated in Fig. 16. By looking at emitters from different parts of the beam, a broadening of the line by several Å is produced because of finite aperture size. Among other things, this broadening smears lines that are close together.

Figure 18 is a schematic diagram of the Meinel spectrograph used at the University of Arizona. It is possible to trace separate colours through the Meinel system and show that blue rays and red rays, due to moving emitters, come through different halves of the optical system. There are obstructions in different parts of the system that can obstruct rays through different paths.

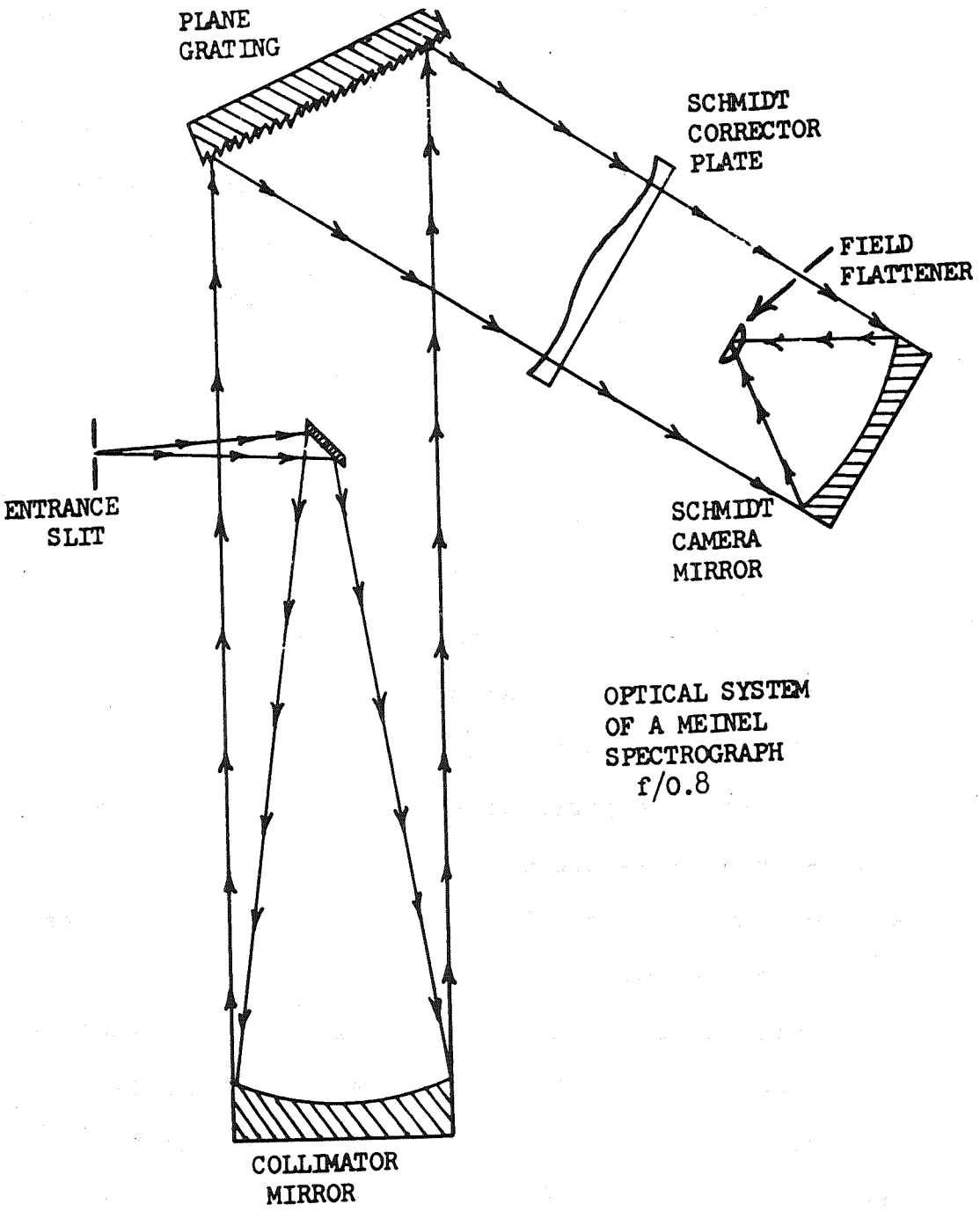

Fig. 18: Diagram of Meinel spectrograph.

These wavelength-dependent obstructions can give asymmetries to the light observed.

The observed effects of this kind of vignetting are illustrated [30,4] in Fig. 19. This is the result of fast moving emitters. To correct the problem it is necessary to blank off part of the collecting region. The determination of the wavelength is affected by the geometries and optical characteristics of the spectrograph used. This must be checked for each individual type of system.

To establish the wavelength of an unknown line it is possible to compare it with the spectrum of a known source, i.e. Fe, Ne, Ar, Hg. The optical system must be carefully checked with these sources. The lines do not fall in the same positions as the beam because they are from emitters at rest. After the known lines have been identified and calibration of the instrument is complete it is possible to compare with the wavelength distribution from the particle beam. When the known wavelengths of the observed beam (either from calculation or previous experiment) are found it is possible, with comparison of standard source, to add or subtract from each line to get the correct wavelength. As stated previously it is hard to get the proper wavelength in the presence of Doppler broadening and vignetting. Vignetting arises when you lose light differentially from some parts of the system.

Perhaps a line is broad because of blending of several lines. These lines may originate from different stages of ionization. It may be possible to solve this

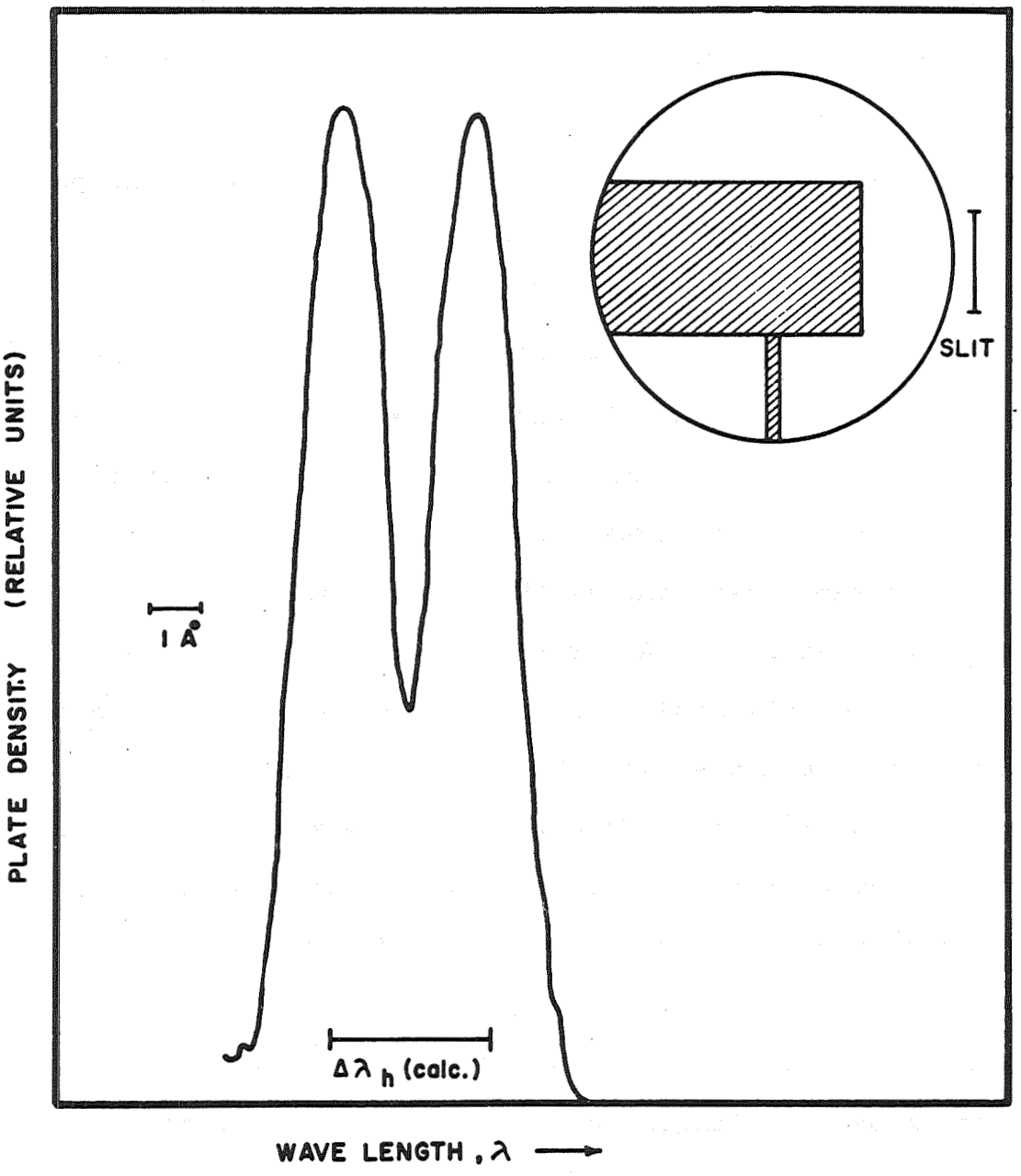

Fig. 19: Effects of vignetting on line shape.

problem by changing the population of the ionization states by changing the energy of the incoming particles. In this way it may be possible to separate the various contributions.

Figure 17 illustrates a proposal [28,29] to reduce the effects of Doppler broadening. Only photons at right angles to the particle beam will be focussed at the entrance slit of the spectrograph. If this is done then only the 90° Doppler shift but no Doppler broadening affects the observed lines. In this system only the non-usable light is bypassed; all good light is collected. It is thought that with this system, broadening of less than 0.05 Å will be observed.

The possibility of very sharp line shapes opens up ideas for new experiments. It would be possible to get j values by splitting lines with a magnetic field and counting the number of component lines. The Zeeman data to date [31] are very poor and new data would be very useful, especially for levels in multiply ionized atoms.

The magnetic field gives a $\vec{v} \times \vec{H}$ force and an associated electric field. This force can move the beam and the electric field can produce a Stark effect. To avoid these effects, it is necessary to send the beam along the lines of the magnetic field to stop these effects. It would be possible to use a super-conducting solenoid.

There are only several labs in the world involved in BFS work. (Note: The number has now risen substantially. See list at end of notes.) There is a

need for ingenuity from new groups. We especially need ideas on how to reduce the broadening of the spectral lines. Two incorrect ways to reduce it are: 1. reduce the size of the input aperture. This reduces the acceptance angle but also reduces the speed of the optical system. 2. reduce the particle speed. This reduces the v/c term but it restricts the ionization distribution.

Question: How much beam is needed?

Answer: The amounts of beam one can use without rapid rupturing of the foils vary but several representative figures can be given: Hydrogen, up to 10 μa. Neon, one-half μa. Iron [7], one-tenth μa. Bromine [32], a few nanoamps. The beams are usually very faint but it must be remembered that all light is usable light; the problem is to get the light out of the system.

There have been effects observed that are produced by a change in foil thickness. The thickness of carbon foils seem to change with time. The relative effects on the total light output have been observed but the differential effects on individual spectral lines are not known.

In many experimental procedures in BFS some method of monitoring must be used. It is possible to accomplish this by collecting the integrated charge. This may not be accurate because changes in foil thickness can produce changes in the ionization distribution which are not proportional to the excitation distribution.

Question: Can you monitor on scattered beam?

Answer: Yes, but solid state detectors are poor for

this purpose. The reason is that heavy ions at low energies give broad, low responses from the detectors.

The best method of monitoring is to look at the light itself. One can use a photomultiplier tube and monitor on the intensity of the beam. A refinement is to use an interference filter and monitor on a particular line. There may be problems in long time intervals with foil thickness changes and replacement of broken foils. The PM tube monitor solves one problem associated with just using integrated charge. When the foil breaks there is no light but there will still be a particle current present.

Initially there was confusion about line broadening from people that were unfamiliar with the BFS technique. In early papers on aluminium [33] and iron spectra the reviewers thought that the lines were too broad and claimed poor experimental technique. The real reason was that there is scattering in the foil. The proposed Axicon system cannot stop the effects of Coulomb scattering; it is necessary to use low Z material foils.

How can one be sure that emitters are what we think? There are several reasons to be assured that a known beam is being observed. 1. Magnetic deflection is used to bend the beam and this brings a clean beam into the target chamber. It is possible to get some contaminants ($N_2 \rightarrow CO$). This can be checked by running possible contaminant spectra and comparing with observed lines or by running monatomic beams (e.g., N).

2. Electric deflection of the beam is used to check contamination. The beam goes through the foil and is then deflected [4,18,20] by parallel plates. The C or O atoms have different velocities than the N so the beam would show a smearing. This smearing has not been seen.
3. Radiation from residual gas may contribute but it can be checked because these atoms give lines that are not Doppler broadened. It is necessary to keep the chamber pressure low. A problem which is associated with the measurement of wavelengths is to determine relative line intensities for such data give information on relative level populations.

Figure 20 illustrates various modes of decay between levels. Consider the d part of that figure and assume level A has the structure $p_{3/2}$, C has $P_{1/2}$ and B has $S_{1/2}$. This is an example of doublet decay. In elementary theory, the rates of decay of the upper levels are identical so the intensities should be of the ratio 1:2 because of relative population. This ratio is expected if the levels are populated according to their statistical weights. There are effects such as configuration interactions, which can cause the upper levels to have different lifetimes. If we assume the two levels have different lifetimes, the measured intensities then depend on the distance downstream at which the beam is observed. For example, let the observations be made at a distance d from the foil. One level has a mean decay distance d_a and the other a mean decay distance d_c. The number of particles in a given level is indicated by N

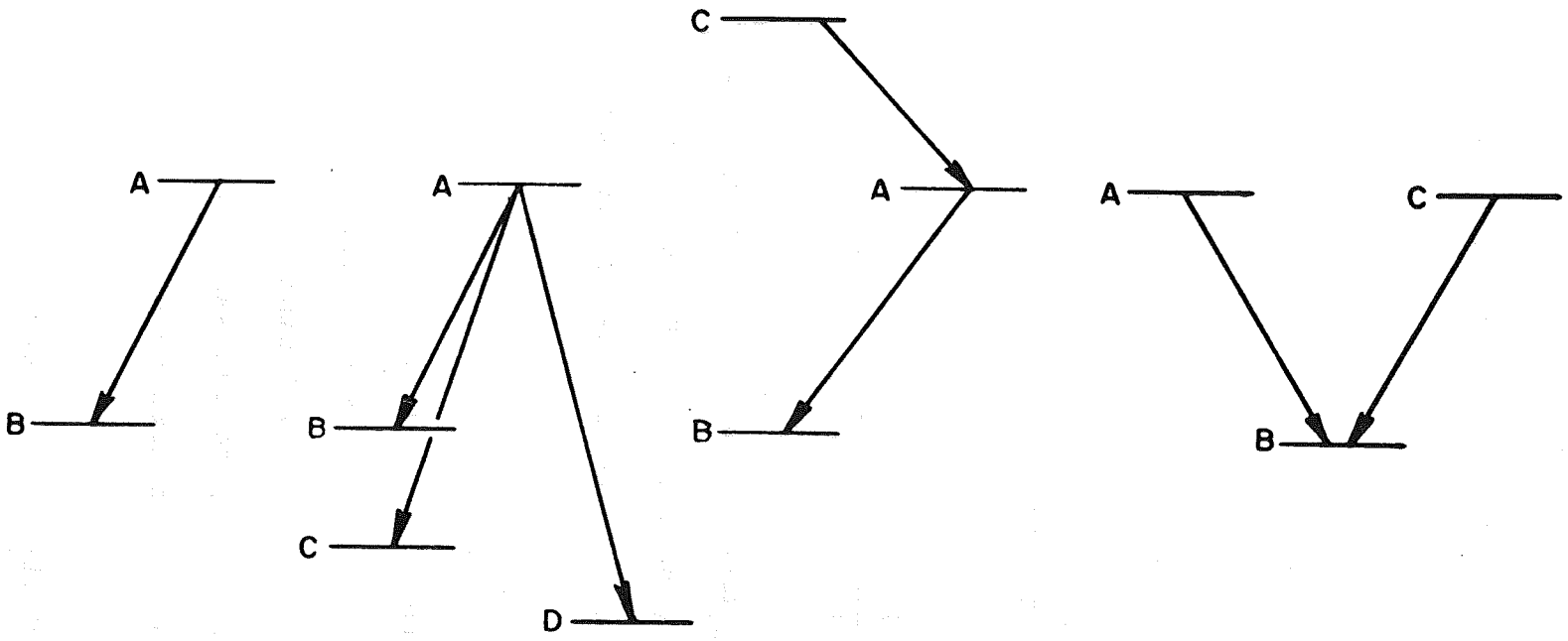

Fig. 20: Illustration of level structures which must be considered in transforming line intensities into population numbers. (a) Isolated level A decays to level B; (b) Level A decays to level B, C, D; (c) Level A is populated by cascades as well as directly; (d) Level A and C decay with different mean lives.

with the appropriate subscript. Then the relative line intensities are given by the following equations:

$$N_a = N_a^o \exp(-t/\tau_a) = N_a^o \exp(-d/v\ 1/\tau_a) = N_a^o \exp(d/d_a)$$

$$N_c = N_c^o \exp(-d/d_c).$$

Since the intensity is proportional to the number of emitters present

$$I \sim N,$$

$$\frac{I_a}{I_c} = \frac{N_a^o \exp(-d/d_a)}{N_c^o \exp(-d/d_c)}$$

$$\frac{N_a^o}{N_c^o} = \frac{I_a}{I_c} \exp\left(\frac{-d(d_a-d_c)}{d_a d_c}\right)$$

Hence measurements of I_a, I_c and the mean decay distances can give the relative level populations. (The problem of the mean decay distances is discussed in the lecture on lifetimes.)

Detectors can be photographic plates or photomultipliers. Photoplates can be used for visible light and for vacuum ultraviolet. It is possible to obtain photomultiplier tubes with special windows to get special fluorescent coatings (e.g., sodium salicylate) to convert the detected radiation to a more compatible wavelength.

Question: What types of lifetimes have been measured?

Answer: 10^{-7} to 10^{-10} second with perhaps 5×10^{-11} as a lower limit. It is now also possible to measure intensities over a length of one meter.

Question: How about measuring hyperfine structure?

Answer: It is impossible with poor line shapes.

Question: Is it possible to look along axis of the beam to reduce Doppler broadening?

Answer: This has been done [34] but a small variation in angle gives a very large effect.

Question: Is there any advantage of integrating along the beam?

Answer: No. You collect the light from any residual gas because the foil is transparent and the beam length is quite long.

Question: Has polarization of the beam been seen?

Answer: There have been two attempts.

1. A polaroid analyzer was placed in front of the photomultiplier tube. The effect may have been too small to observe in this crude measurement where integrated light was detected.

2. In one measurement a spectrograph was used to get a spectral analysis. It was found that the light was polarized. However, light from any dielectric surface will be polarized, and the entire effect came simply from the grating.

(Carriveau and I have succeeded in observing polarization of beam light in Stark effect experiments carried out after these lectures were delivered.)

A curious and extremely interesting feature of BFS is that new spectral lines, never previously reported are often seen even in well-studied elements. Nitrogen [5] shows perhaps twenty such lines, sodium [6] nearly 100 and

fluorine and sulfur [35] numerous others. These lines are often the strongest in the spectrum. The states from which they come are wholly unknown, although we have found their lifetimes to be of the same order as those of known states. In some cases [6,7,20], the charge of the parent emitters has been determined.

LIFETIME MEASUREMENTS

DEFINITION OF TERMS

Level: Characterized by energy, spin, orbital angular momentum, and total angular momentum.

This would not be called a state because a state is the most refined term. For example, the level $4S\ ^3P^o_2$ has five magnetic sub-states. In the present work, it is most practical to talk about levels and not states.

Figure 21 shows a transition array containing two multiplets. The selection rules for the transition are: $\Delta\ell = \pm 1$, $\Delta j = \pm 1$ or 0 but the transition from 0 to 0 is not allowed.

The mean life of each level is independent of angular momentum j if there is no configuration mixing. Configuration interactions for close multiplets can occur [36].

Intensity of transition: The intensity of the transition from level A to B may be written [37]

$$I(A,B) = c_1 \sum_{a,b} |(a|P|b)|^2$$

where c_1 is a constant and a and b are levels contained in the multiplets A and B. P is the electric dipole operator.

The summation in the expression is called the strength of the transition

$$S(A,B) = \sum_{a,b} |(a|P|b)|^2$$

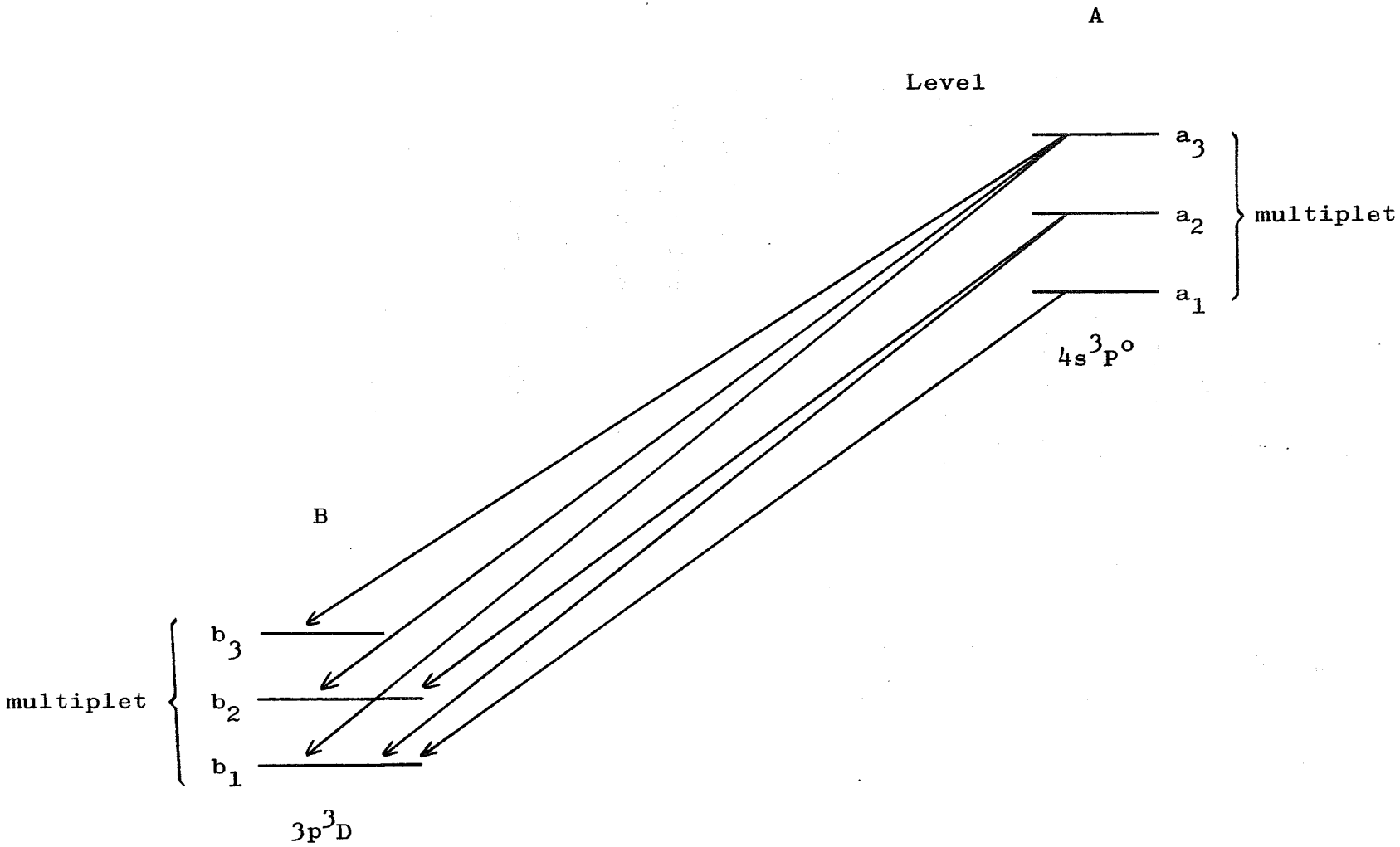

Fig. 21: Transition array with two multiplets.

There are also the strengths of separate transitions or partial strengths:

$$S(a,B) = \sum_b |(a|P|b)|^2$$

$$S(A,b) = \sum_a |(a|P|b)|^2$$

It follows that

$$S(A,B) = \sum_a S(a,B) = \sum_b S(A,b)$$

The transition probability per second or Einstein A coefficient is written

$$A = \frac{c_2 S(A,B)}{2J_A + 1}$$

where c_2 is a constant and the denominator is the statistical weight. This coefficient has units of $(\text{time})^{-1}$. It is asymmetric in the levels A and B because of the statistical weight factor.

The oscillator strength, f(a,b), is related to the strength of the transition from a to b by

$$f(a,b) = \frac{c_3 S(a,b)}{2J_b + 1} ;$$

c_3 is a constant. Because of the statistical weight, the oscillator strength is not symmetrical in a and b. By definition the oscillator strength is positive for absorption. Induced emission (negative absorption) is then described by a negative oscillator strength and

$$(2_{jb}+1)\ f(a,b) = -(2_{ja}+1)\ f(b,a)$$

We are concerned with the total probability of

decay of a level i

$$A_i = \sum_{f<i} A_{if} = \frac{1}{\tau_i}$$

where the summation is over all final levels with energy less than the initial levels. The term τ_i is called the mean life of level i.

The intensity in a line is given by

$$I_{if} = N_i(t)\ A_{if}$$

where $N_i(t)$ is the (time-dependent) population of level i.

The power output in the transition from i to f is

$$P_{if} = h\nu_{if}\ I_{if}(t)$$

where $I_{if}(t)$ is the number of photons per second and may be time-dependent.

$$P_{if} = h\nu_{if}\ A_{if}\ N_i(t)$$

Consider, as shown in Fig. 22, a level with several modes of decay. Our measurements, even if they are made on only one of the allowed modes of decay, give us the mean life of level B. If one wants to know the fraction of decays in each decay mode, one must also determine the relative line intensities. When, as often happens, the lines are in widely different parts of the spectrum, this is rather hard to do. We would like to get the total transition probability per second.

Suppose there are other levels which decay from a higher energy to the level that is being studied. Then there is a cascade [16] to the level in question. Perhaps

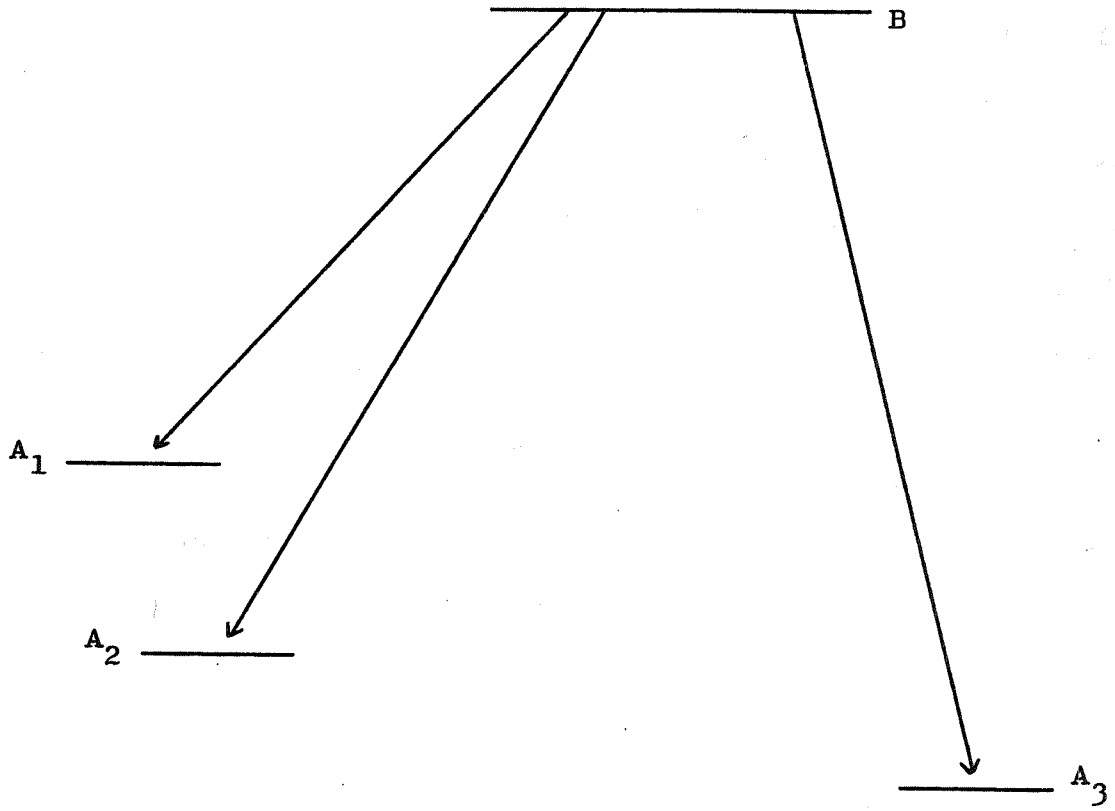

Fig. 22: Assumed level showing several modes of decay.

the level is not populated in the foil but is populated solely by cascades from other levels. One then expects to see a maximum in intensity some distance downstream from the foil depending on the lifetimes of the upper levels. (Actually such an intensity variation has not yet been seen.) In a paper to be published from Arizona, an example of such a decay is given. See ref. 9. Cascades may produce various peculiarities in the data.

Figure 23 shows part of the Balmer series in hydrogen. In this case the lines are from contributions from different (degenerate) levels. The mean lives are different for the S, P and D modes. The decay curve depends on the mean lives and how the component levels were populated. Things can get very complicated when there are cascades and degeneracy.

The data [38] taken from hydrogen are shown in Fig. 24. As can be seen, there are two lifetimes involved and fitting is done using a computer program and subtracting the longer lifetime. In this work, the contribution from the P level is not seen; only the 3S and 3D contributions can be found.

Figure 25 shows the Lyman α line. Here there are only two contributions [39] to the decay. There is however a substantial cascade to the 2P levels from n = 3 above, as the 2S level is populated either directly at the foil or from cascades. It is also possible, through a small field [23,27], to produce transitions from the metastable 2S level to the 2P levels. Hence the analysis of the Ly α decay curve is pretty complicated.

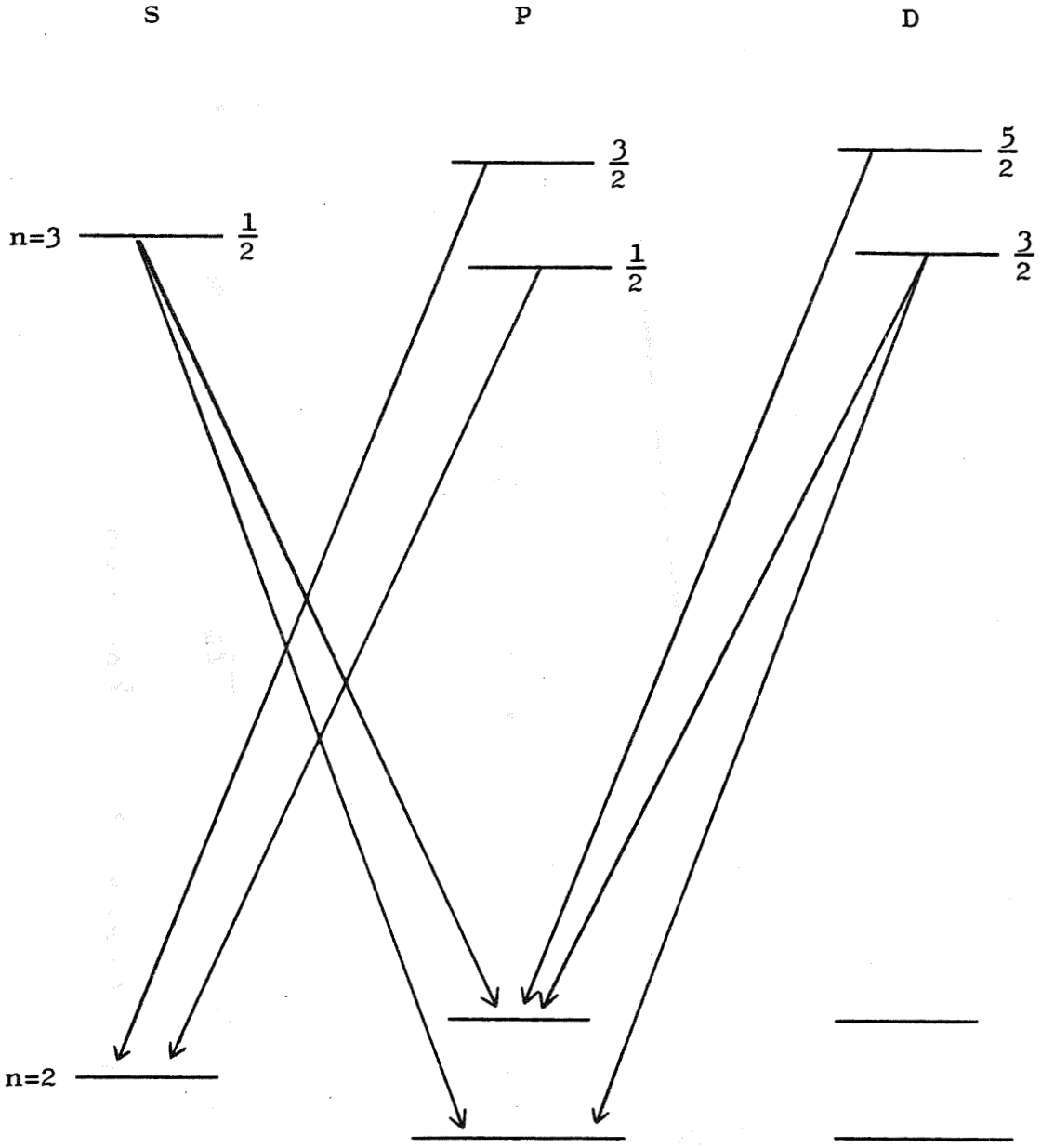

Fig. 23: H_α Balmer line in hydrogen.

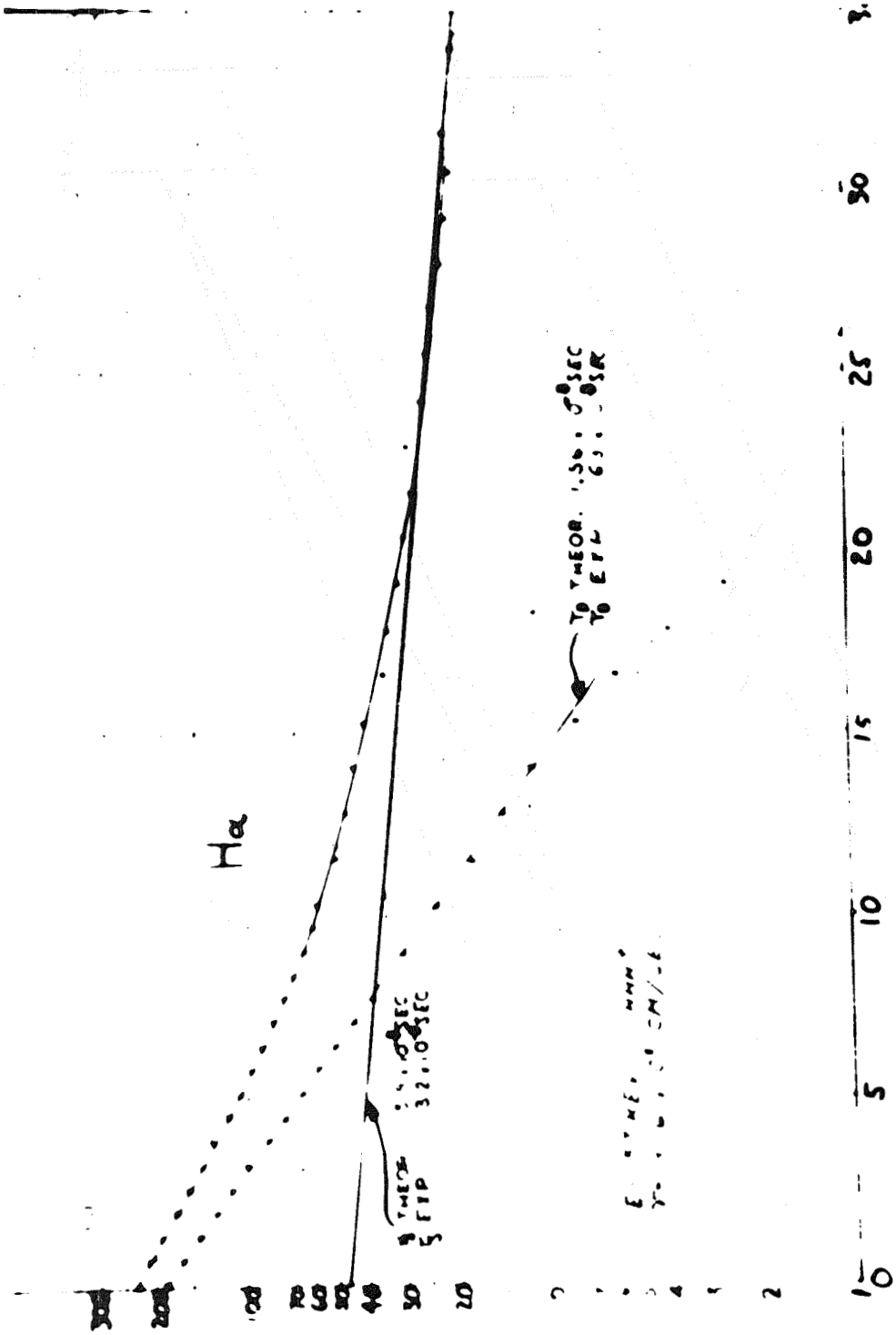

Fig. 24: Results from data taken on H_α line in hydrogen.

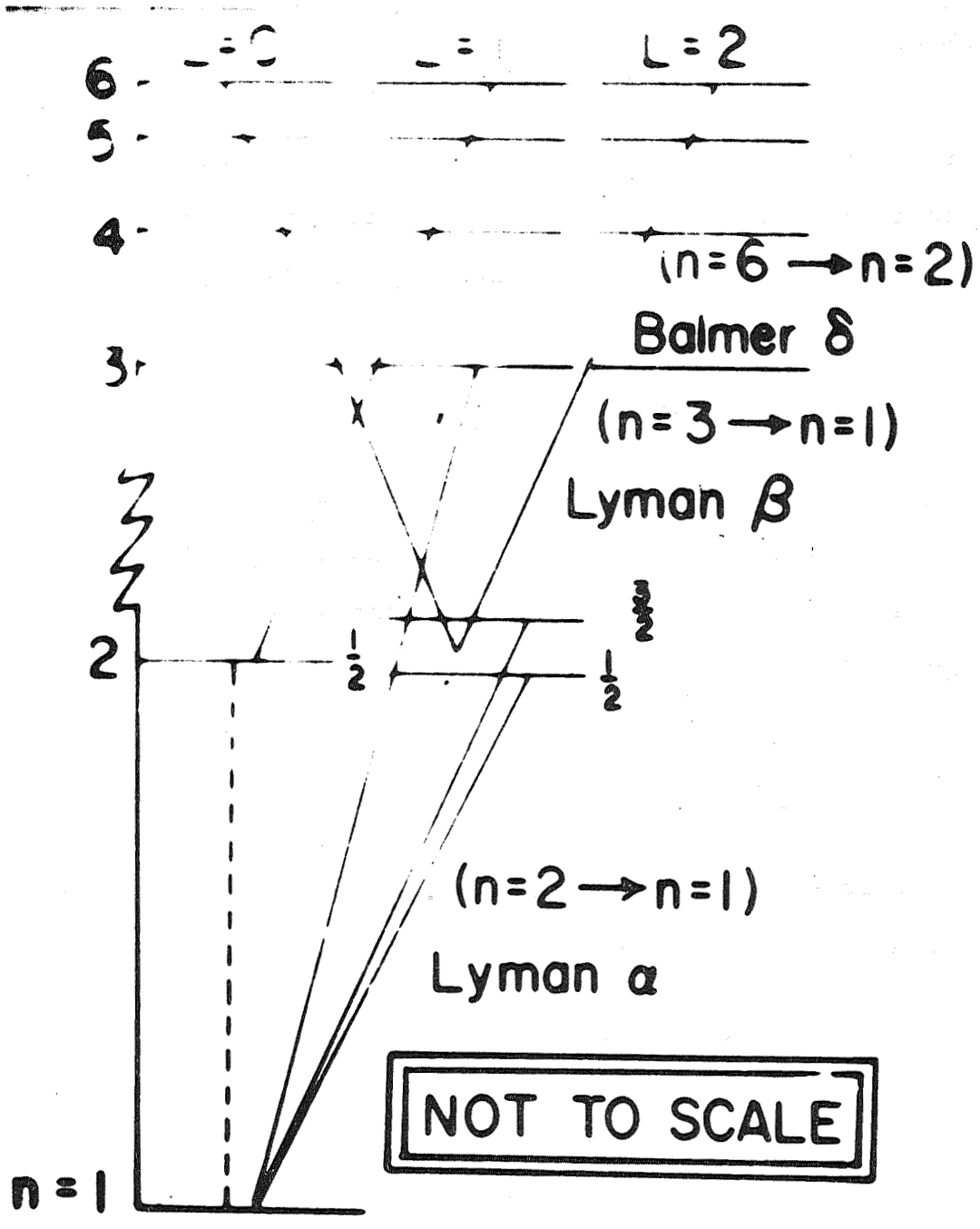

Fig. 25: Lyman α sequence showing cascades.

Another example of different lived components is shown in Fig. 26. Long lived components are seen in the tail of the curve; these components are from cascades and Stark mixing.

One can write the equation for the decay of excited states as a function of time. The number of decays per unit time is proportional to the number in the initial state and the sum of the transition probabilities

$$\frac{dN_i}{dt} = -N_i \sum_{f<i} A_{if}$$

where the sum is over all final states with energies less than the initial state. If there is population by cascades from states with energy higher than the initial state energy it is necessary to add a term

$$\frac{dN_i}{dt} = -N_i \sum_{f<i} A_{if} + N_j \sum_{j>i} A_{ji}$$

In the first case, with no cascades, one solution to the differential equation is

$$N_i(t) = N_i(0) \exp\left(\sum_{-f<i} \right) A_{if} t$$

$$= N_i(0) \exp\left(-\frac{t}{\tau_i}\right)$$

Remembering that the radiating particles are travelling at a constant velocity this may be written

$$N_i(t) = N_i(0) \exp\left(-\frac{d}{v\tau_i}\right)$$

where d is the distance downstream from the foil.

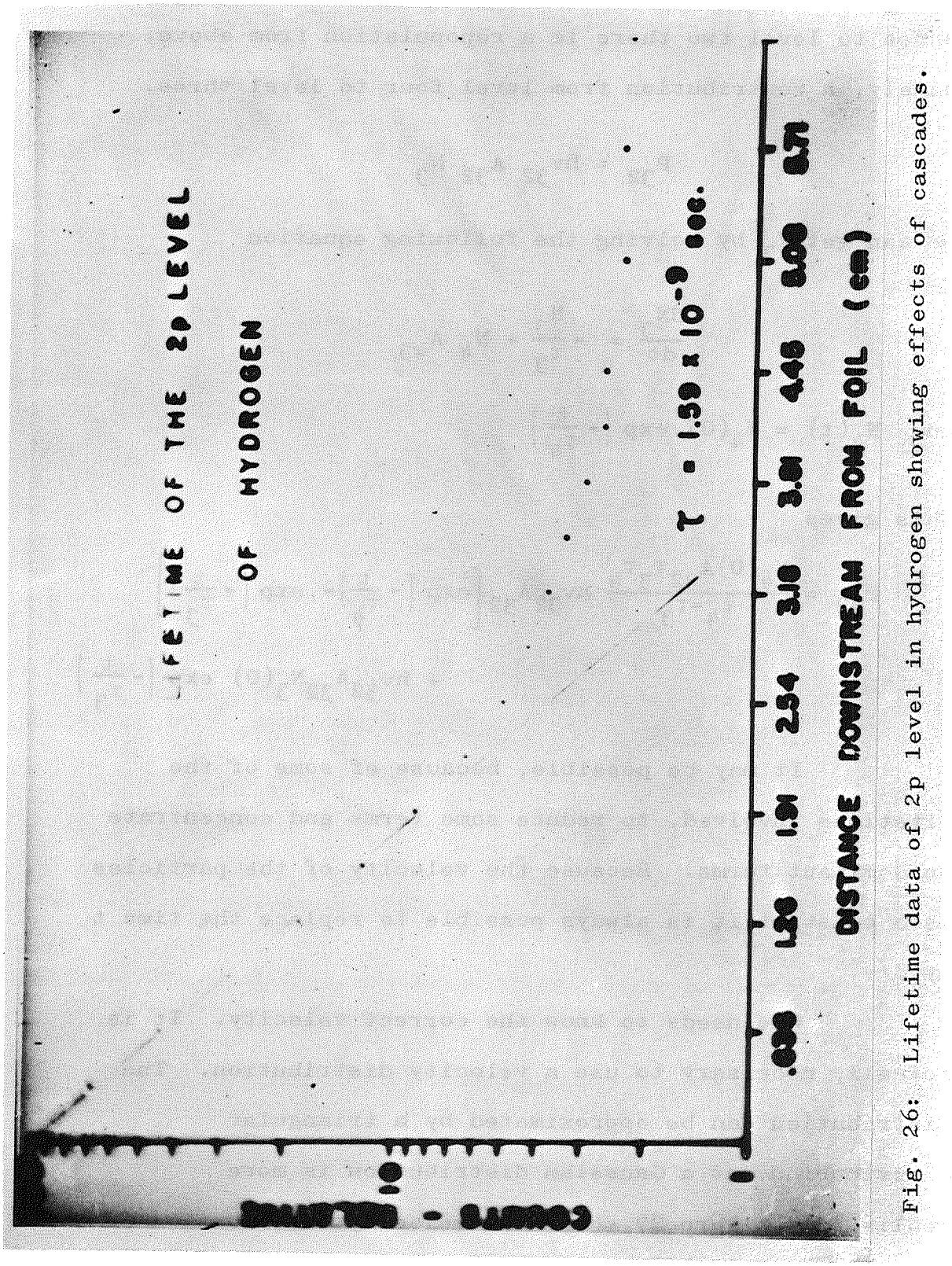

Fig. 26: Lifetime data of 2p level in hydrogen showing effects of cascades.

Consider a system with four steps of decay. Assuming that level four (the highest in energy) is not populated from cascades, then only the decay from level four shows a simple exponential. For decay from level three to level two there is a repopulation from above; namely, a contribution from level four to level three.

$$P_{32} = h\nu_{32} A_{32} N_3$$

we can get N_3 by solving the following equation

$$\frac{dN_3}{dt} = -\frac{N_3}{\tau_3} + N_4 A_{43}$$

and $N_4(t) = N_4(0) \exp\left(-\frac{t}{\tau_4}\right)$

This gives

$$P_{32} = \frac{N_4(0)A_{32}\tau_3\tau_4}{\tau_4-\tau_3} h\nu_{32}A_{32}\left[\exp\left(-\frac{t}{\tau_4}\right) - \exp\left(-\frac{t}{\tau_3}\right)\right] + h\nu_{32}A_{32}N_3(0) \exp\left(-\frac{t}{\tau_3}\right)$$

It may be possible, because of some of the lifetimes involved, to reduce some terms and concentrate on dominant terms. Because the velocity of the particles is a constant it is always possible to replace the time t by d/v.

One needs to know the correct velocity. It is actually necessary to use a velocity distribution. The distribution can be approximated by a triangular distribution but a Gaussian distribution is more realistic. Figure 27 shows the velocity distribution of Be III before and after passage through a thin C foil.

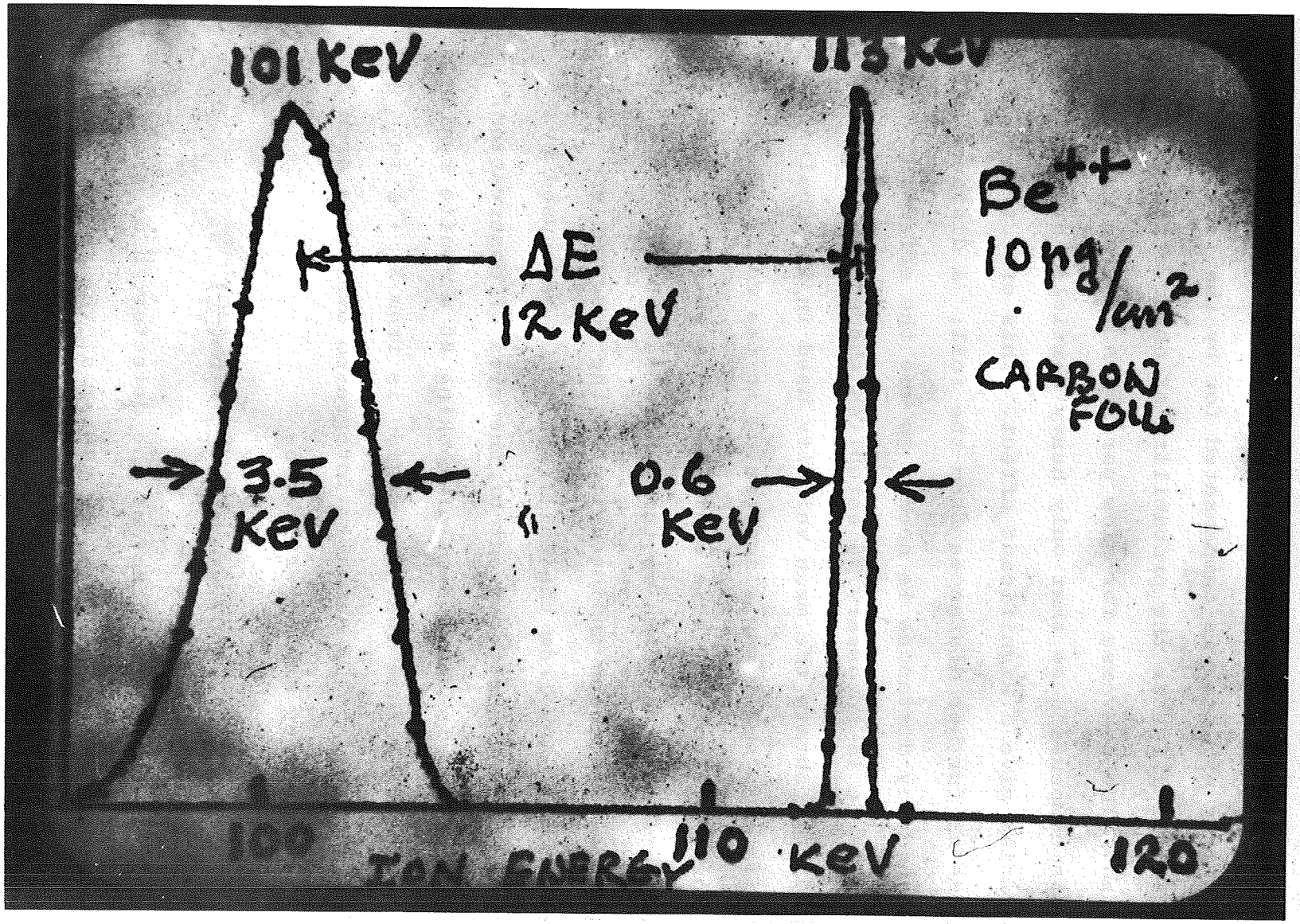

Fig. 27: Energy distributions in Be before and after passage through thin carbon foil.

The energy is shifted by 12 keV and the width at half maximum changes by about a factor of 6.

Particles arriving at the point of observation too soon give a greater intensity. The enhanced probability of decay is compensated for by the fact that in travelling faster the probability of observation is reduced. The converse for slow particles is true. These effects compensate so that only heavy particles at slow velocities give a significant effect. This effect is more obvious at further distances from the foil; a distance of 10 mean decay distances is needed to see the effect.

It is necessary to establish the energy lost in the foil to obtain the mean velocity used in the analysis. There is also small angle scattering in the foil. Because the analyzer looks at some small finite area of the beam, great care must be taken so that there is not an artificial reduction in intensity as the observation points moves away from the foil. This may be caused by particles being scattered out of the area of observation.

What is the effect of looking at a finite region of the foil? Assume that the region is from $X_o + \Delta$ to $X_o - \Delta$. The light is actually integrated over this area and the intensity can be written as

$$I \sim E(\lambda)\Omega\ N(0)\ v\ \exp\left(-\frac{X_o}{v\tau}\right)\ \sinh\left(\frac{\Delta}{v\tau}\right)$$

where $E(\lambda)$ is the efficiency of the detector, Ω is the geometrical factor, $N(0)$ is the number at the region, and τ is the mean life of the state.

It is necessary to know if the same number of

particles are produced at the foil for each increment of time as time passes. The foil thickness may change in time and time-dependent effects of light output have certainly been seen. It is necessary to use a monitoring system. If a Faraday cup is used the geometry of the system should remain the same to reduce the effect of scattering beam out of the cup as the foil is moved.

Figure 28 illustrates the ionization states of H_2F^+. As can be seen there are large contributions from two, three and four ionization stages but also some contribution from up to nine times ionized. One can adjust the distribution in each experimental case by changing the energy of the incoming particles. One can obtain very high ionization states, even up to the forty-second ionization state of uranium [40].

A spectrum from lithium [41] is shown in Fig. 29. While many peaks are seen, some peaks are very strong. These have been found to originate from two electron transitions. These multi-electron levels have lifetimes that are in either good or very poor agreement with theory.

An example of a line that is derived from multiply excited states is shown in Fig. 30. Two components are separated in each case.

The mean life of the decay of a N V doublet [13] is shown in Fig. 31. The levels should have the same lifetime but the intensity depends on the energy.

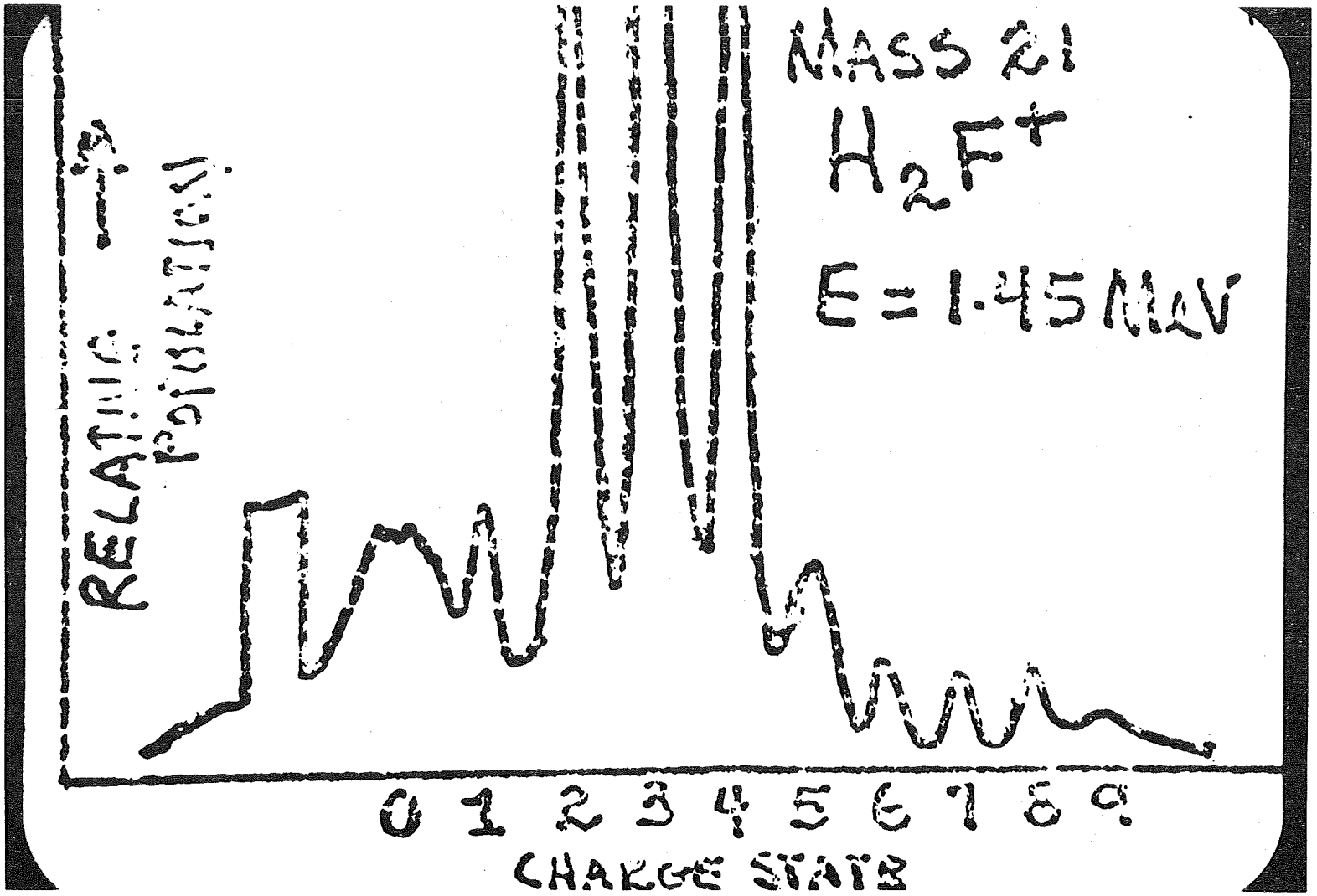

Fig. 28: Relative population of ionization stages in H_2F^+ after passage through thin foil.

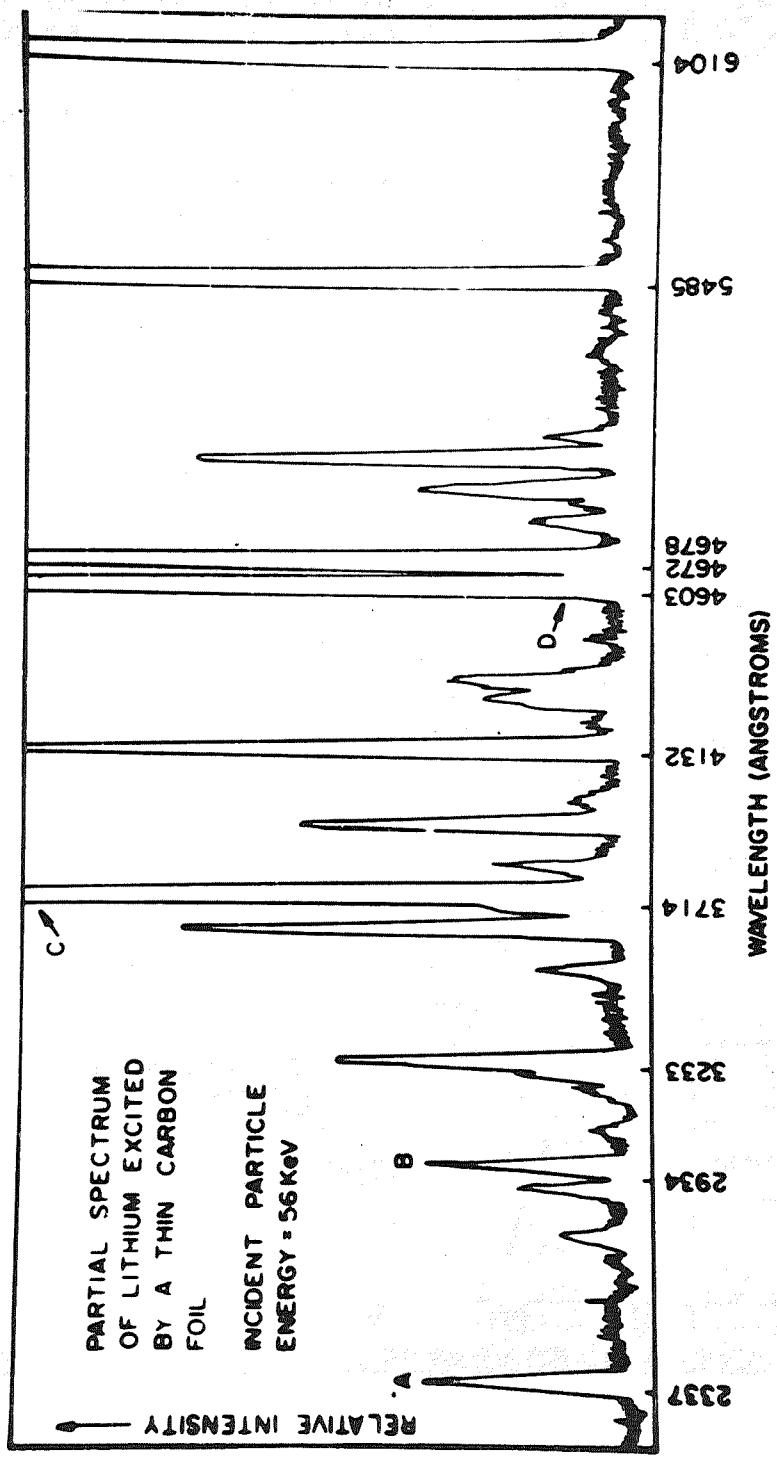

Fig. 29: Spectra of Li.

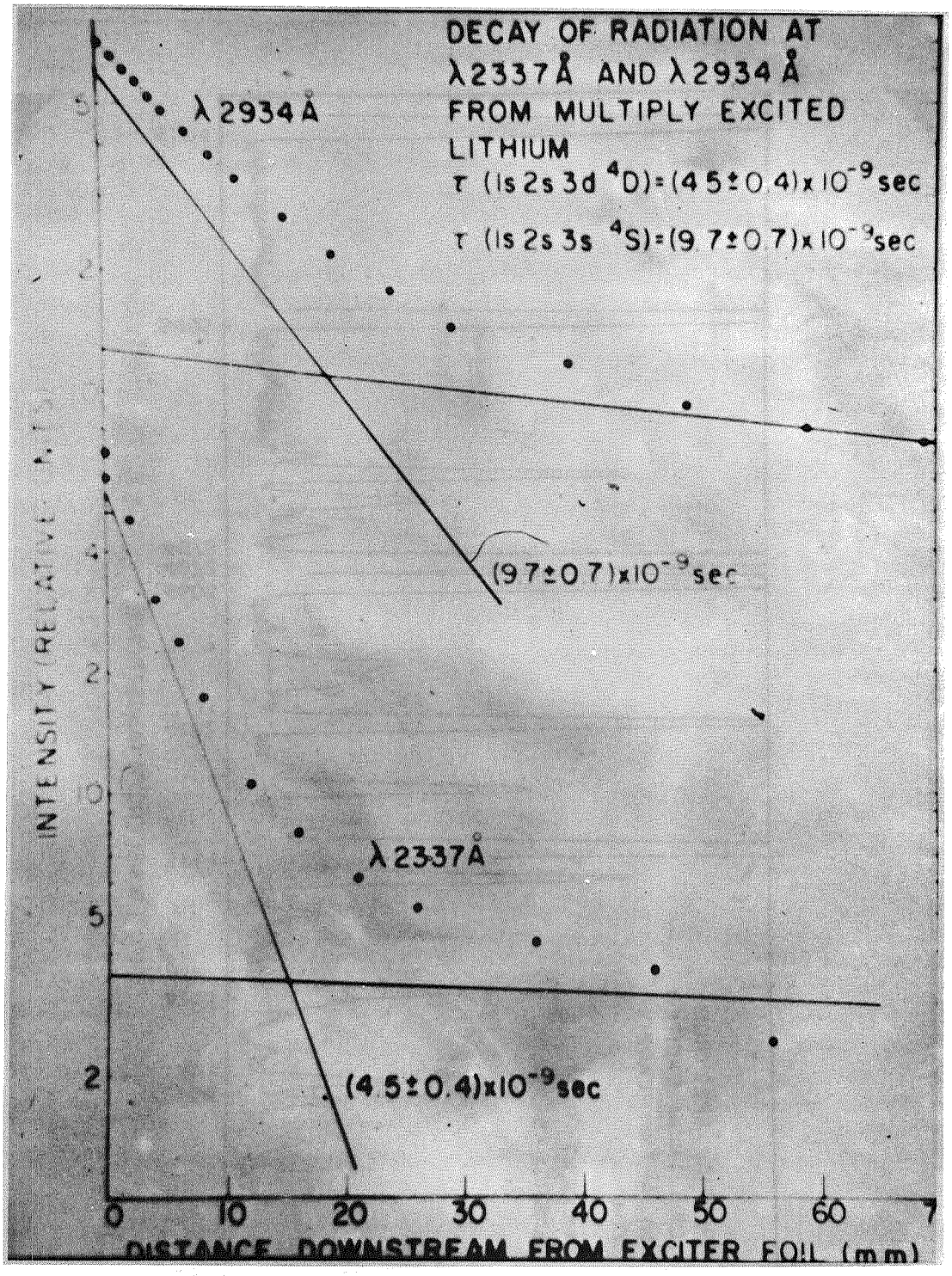

Fig. 30: Lifetime data and determination for Li.

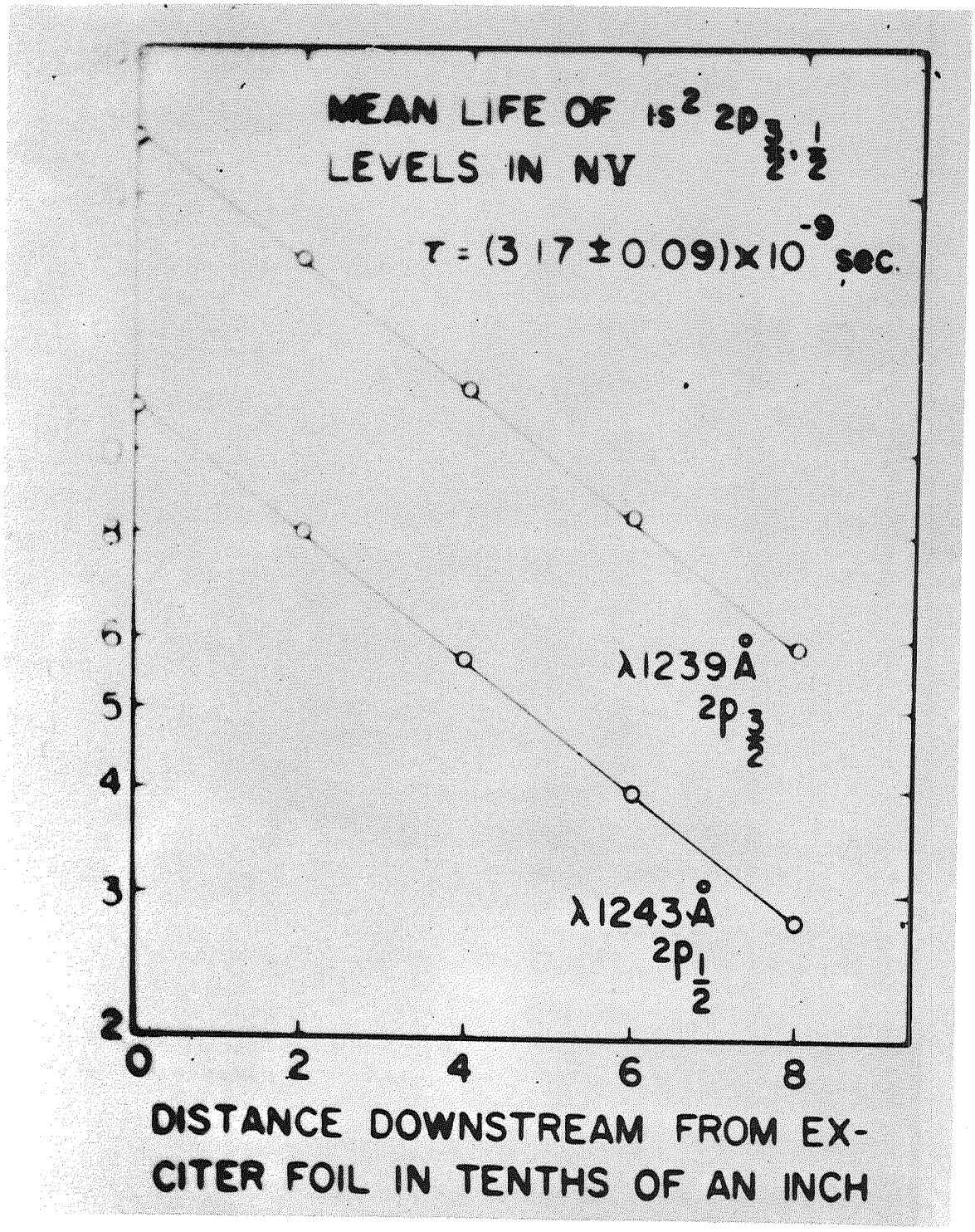

Fig. 31: Mean life of a N V doublet.

APPLICATIONS

By using the BFS method, there are many measurements that can be made but some are more interesting than others. This lecture will cover certain applications of the BFS method, especially in astrophysics.

One can study the variety and relative abundance of elements in the universe. The general distribution [42] is the same everywhere. One must use relative element abundances in formulating theories of creation and structure of the universe and creation of chemical elements. If, for example, an assumption is made that stars are composed of radioactive material, they should contain the well-known decay products. These have not been seen. Also, if radioactive, then there should be noticeable effects on the power output, the lifetimes, and the ages of stars, but these effects are at variance with the data. Thus the analysis of stellar life is critically dependent on the observations of the relative abundance of elements.

How do people decide on abundances? [43] Astronomers study intensities of the spectral lines emitted by stars and other astronomical light sources. These spectra are usually continuous (hot body) with absorption dips (from the stellar atmosphere). Comparison of the wavelengths of these dips with known absorption spectra establish the composition of the stars.

To obtain abundances, one looks at the depth of the dips in the absorption profile; this depth is

essentially proportional to the abundance. One must also take into account the characteristics of the atmosphere under study. The number and types of energy levels that atoms of the atmosphere may exhibit depends on, among other things, the temperature of the surface of the star, the electron pressure, and the density. These characteristics are astrophysical and can be calculated from stellar models. The depth in the absorption profile also depends on the types of atoms themselves and this is the factor of concern to us.

Consider the rate of radiation from a level. If the level lifetime is short, the number of emitters in that level will decay rapidly. In statistical equilibrium, a condition which exists in stellar atmospheres, the particles will be rapidly re-excited to that level. Hence there will be a substantial dip in the continuum, essentially because there are always particles capable of absorbing light of the appropriate wavelength. On the other hand, a long level lifetime means that the number of particles able to absorb that light is reduced. Hence the depth of the absorption profile is greater for short-lived levels than for long-lived levels, all other factors remaining constant. For this reason, the measurement of level lifetimes is an important aspect of the problem of determining element abundances. With BFS, one can directly measure such lifetimes, not only in atoms, but also in monatomic ions, which are also significant in many stars. In the following, it is convenient to discuss transition probabilities instead of level lifetimes, but they are

related by

$$A = \tau^{-1} .$$

There has been only one application of this method to date, since most work has been done towards development of experimental techniques. The published work has been done with iron at Cal Tech. Iron is the element of most significance to astrophysicists. There is a great increase in relative abundance of the elements near the iron region, perhaps by a factor of 1000.

Why are the iron and near iron elements so much more abundant? Speculation gives theories [42,44] of production of the elements. There is a need of medium weight elements for seeds for neutron absorption. How does the iron group fit? ^{56}Fe is the most stable of all nuclides. Under certain supernovae conditions there is a great squeezing of the existing elements which produces a high temperature and density. This equilibrium process gives an increase in iron groups.

It is possible to measure transition probabilities in the lab. One method is to use a carbon arc [45] and iron and produce an absorption spectrum. There is one problem: the coefficients obtained by this method can be off by a factor of 5. Precisely this difference was seen by comparison with Cal Tech results using BFS. Specifically the average transition probabilities measured at Cal Tech are 5 times smaller than the U.S. Bureau of Standards' data. This means that the iron abundance in the sun must be raised by this factor of 5.

Some stars seem to have an overabundance of rare-earths. However, the transition probabilities may be off by a factor of 1000. These probabilities should be carefully measured using BFS methods. Another place where BFS can be of great utility is in obtaining oscillator strengths. Consider a level which has several modes of decay. Perhaps only one of them is in a spectral region - say the visible - which enters into an astrophysical problem. It is no longer sufficient just to measure the level lifetime, since

$$\tau^{-1} = \sum_{i<k} A_{ik}$$

where k is the level of concern, i represents all the levels to which decays are permitted, and only one particular value of i, say I, is interesting. The astronomer describes the contribution of decay I_k in terms of the absorption oscillator strength,

$$f_{Ik} = \frac{\text{const x } S(I,k)}{(2J_k+1)} ,$$

where J_k is the total angular momentum of the upper level and S(I,k), the strength of the transition, is related to the transition probability through the operations

$$A = \text{const} \sum_i \frac{S(i,k)}{(2J_i+1)} .$$

To find S(I,k) from A, one must also know the 'branching ratio', or the fraction of the level decays that lead to level I. This means measuring the relative intensities of all the transitions k → i.

Such measurements may be quite difficult with

ordinary light sources since the several transitions may involve wavelengths in widely different parts of the spectrum - perhaps the extreme ultraviolet and the visible. With BFS, however, such measurements are straightforward, and one need correct only for detection efficiency vs. wavelength. It is worth noting that such measurements can be made at any convenient downstream position.

A rather different type of astrophysics has to do with Quasers. In the study of Quasers a line like Lyman α is seen. This is thought to be explained [46] because the objects are moving away so fast that the Doppler (red) shift brings Lyman α (1216 Å) into the visible. In Quasars, one may see [47] a dozen lines that cannot be identified from conventional sources unless they are Doppler shifted. Thus, Quasars give sets of strange lines. While sharp in emission, they may have absorption profiles 100 Å wide. Thus it is not easy to be sure that the correct wavelength assignments have been made. Moreover, it seems that a single Quasar may have several red shifts [46].

Now, as emphasized in the talk on wavelengths, BFS studies of elements have also given many unexplained lines. We do not know from what levels these new lines emerge. My point is that, until we have a good explanation of the origins of those strange lines, one should be a bit cautious in assigning extraordinary properties to the sources of the strange lines detected in Quasars.

It is not possible to say the lines are the same as those from Quasars but a thorough study of the beam-foil

excitation process may give insight into other processes. A systematic survey of common elements is needed.

Still another application of BFS is in connection with the composition of the solar corona. That spectrum contains wavelengths from atoms in highly ionized states, and only about half [48] of the lines have been identified. Since BFS makes it possible to get nearly every ionized state from most elements, one can hope to use the laboratory studies to clarify the corona. One good identification, in Ne VII, has already been reported [11]. An experimental measurement of comparison spectra for solar corona studies is needed.

As a final illustration of the application of BFS, consider the theoretical work on transition probabilities. In recent years, there has been a major search [14] for regularities in transition probabilities. Such a search was not practical earlier because of the scarcity of data. Needless to say, the regularities which have been seen in experiments have been interpreted by means of calculations according to various models.

In Fig. 32, we see a comparison [14] of experimental and calculated values, and one sees that there is pretty good agreement. On the other hand, Fig. 33 shows that serious discrepancies [49] can arise. Over half the data in Figs. 32 and 33 come from BFS. It is clear that the opportunity to examine a given transition over a wide range of nuclear charges, i.e., over an isoelectronic sequence, makes BFS of special value in corroborating or correcting the theoretical models.

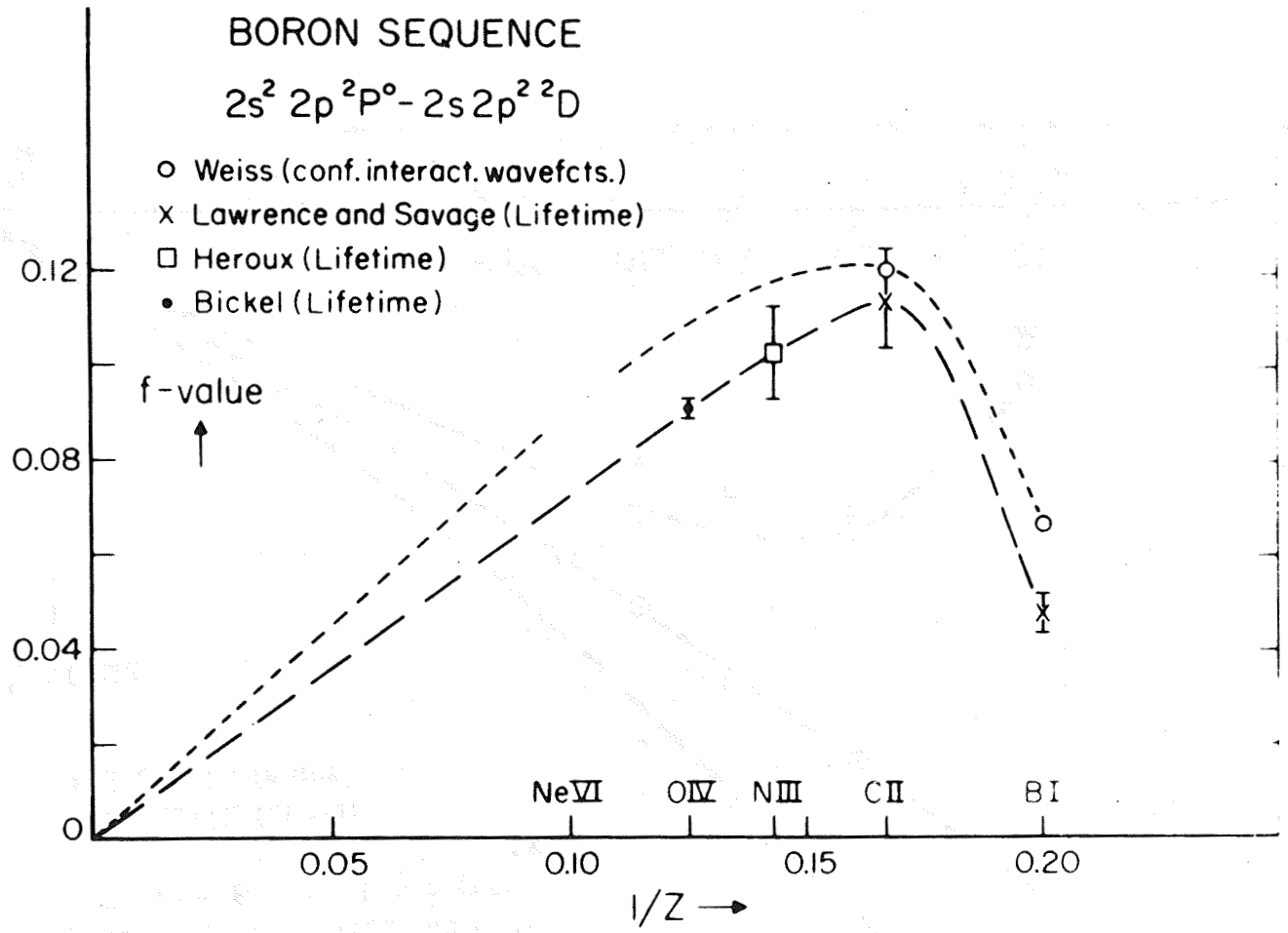

Fig. 32: Dependence of f-value on 1/Z for the $2s^2 2p\ ^2P^o - 2s2p^2\ ^2D$ transition of the boron sequence.

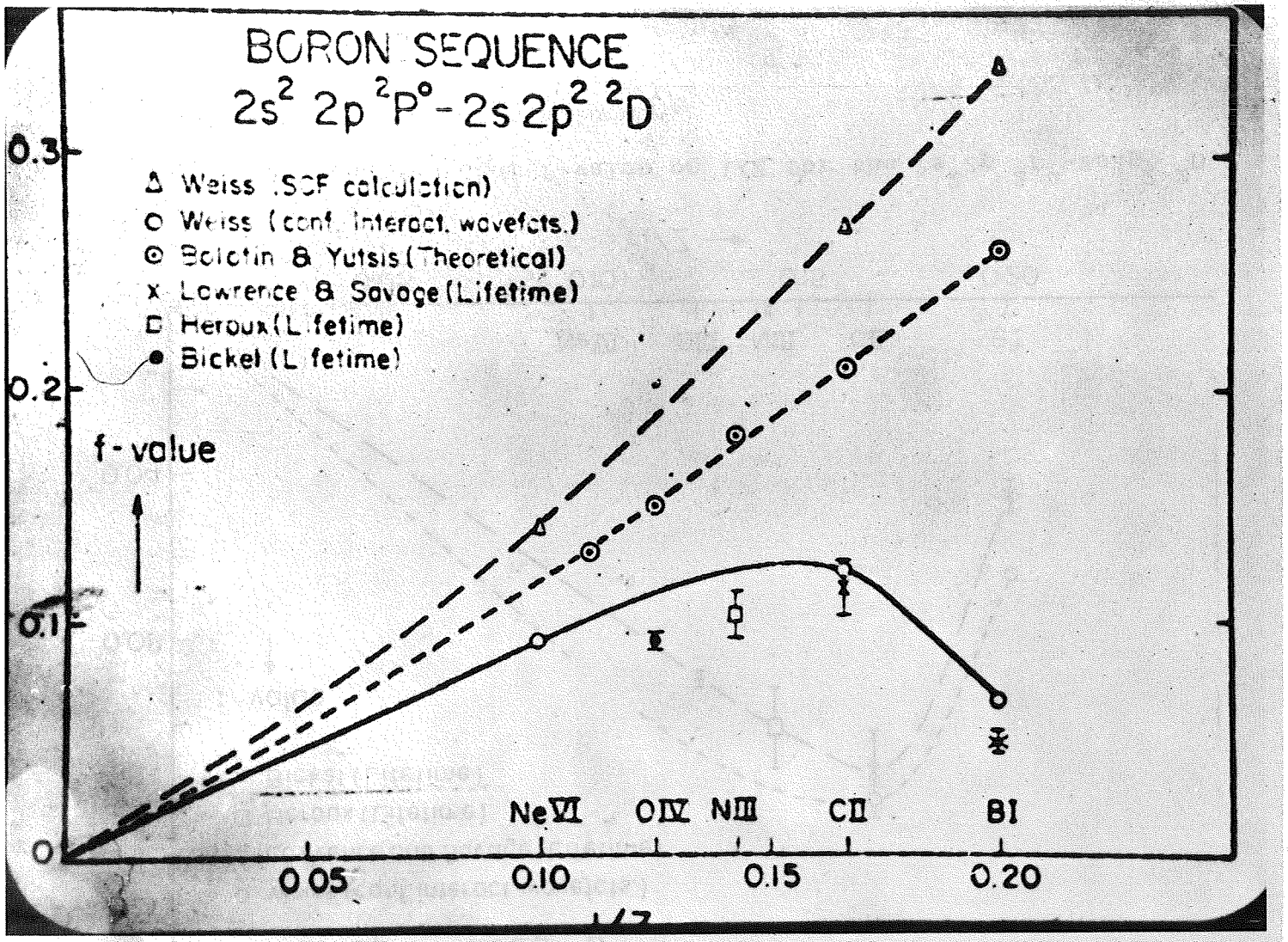

Fig. 33: Dependence of f-value on 1/Z for the $2s^2 2p\ ^2P^o - 2s2p^2\ ^2D$ transition of the boron sequence.

REFERENCES

1) S. Bashkin, A. Malmberg, P. Meinel, and S. Tilford, Phys. Lett. 10, 53 (1964

S. Bashkin, P. Meinel, Astrophys. J. 139, 413 (1964)

2) S. Bashkin, Nucl. Instr. and Meth. 28, 88 (1964)

S. Bashkin, Science 148, 1047 (1965)

3) W.S. Smith, unpublished M.S. Thesis work, U. of Arizona

4) S. Bashkin, Beam-Foil Spectroscopy (Gordon and Breach, New York, 1968)

5) U. Fink, G. McIntire, and S. Bashkin, J. Opt. Soc. Amer., 58, 475 (1968)

6) L. Brown et al., Beam-Foil Spectroscopy (Gordon and Breach, New York, 1968)

7) W. Whaling et al., Beam-Foil Spectroscopy (Gordon and Breach, New York, 1968)

8) S. Bashkin, B. Curnette, and W. Bickel (unpublished)

9) Berry et al., to be published

10) L. Heroux, Beam-Foil Spectroscopy (Gordon and Breach, New York, 1968)

L. Heroux, Phys. Rev. 153, 156 (1967)

11) S. Bashkin, L. Heroux, and J. Shaw, Phys. Lett. 151, 87 (1966)

12) W. Bickel and S. Bashkin, Phys. Lett. 20, 488 (1966)

13) W. Bickel, R. Girardeau, S. Bashkin, Phys. Lett. 28A, 154 (1968)

14) W. Wiese, Beam-Foil Spectroscopy (Gordon and Breach, New York, 1968)

15) W.S. Bickel, H.G. Berry, I. Martinson, R.M. Schectman, S. Bashkin, Phys. Lett. 29A, 4 (1969)

16) L. Heroux, Phys. Rev. 161, 47 (1967)

17) E.U. Condon and G.H. Shortley, 'The Theory of Atomic Spectra' (Cambridge Press, London, 1963)

18) P. Malmberg, S. Bashkin, and S. Tilford, Phys. Rev. Lett. 15, 98 (1965)

19) Frontispiece B., Beam Foil Spectroscopy (Gordon and Breach, New York, 1968)

20) U. Fink, J. Opt. Soc. Amer. 58, 937 (1968)

21) G. Carriveau, S. Bashkin, H. Hay, 41st ANZAAS Congres (1969)

22) S. Bashkin, G. Carriveau, H. Hay (to be published)

23) S. Bashkin, W. Bickel, D. Fink, and R. Wangness, Phys. Rev. Lett. 15, 264 (1965)

24) S. Bashkin and G. Beauchemin, Can. J. Phys. 44, 1603 (1966)

25) W. Bickel and S. Bashkin, Phys. Rev. 162, 12 (1967)

26) R. Wangness, Phys. Rev. 149, 60 (1966)

27) I.A. Sellin, G.D. Moak, P.M. Griffen and Biggerstaff, Phys. Rev. (to be published)

28) S. Bashkin, Beam Foil Spectroscopy (Gordon and Breach, New York, 1968)

29) J.O. Stoner, (to be published)

30) L.C. Marquet, J. Opt. Soc. Amer. 57, 878 (1967)

S. Bashkin, Appl. Opt. 7, (Dec. 1968)

31) Moore, on Zeeman data

32) G.D. Moak et al., Beam Foil Spectroscopy (Gordon and Breach, New York, 1968)

33) S. Bashkin et al. J. Opt. Soc. Amer. 57, 1395 (1967)

34) J.A. Jordan, Jr., Beam Foil Spectroscopy (Gordon and Breach, New York, 1968)

A. Denis et al., Beam Foil Spectroscopy (Gordon and Breach, New York, 1968)

35) Univ. of Arizona BFS group, (to be published)

36) W.L. Wiese, M.W. Smith, and B.M. Glennon, Atomic Transition Probabilities, Vol. 1, Hydrogen through

Neon, NSRDS-NBS 4 (1966)

37) see ref. 17, page 98

38) A.S. Goodman and D.J. Donahue, Phys. Rev. 141, 1 (1966)

39) W.S. Bickel and A.S. Goodman, Phys. Rev. 148, 1 (1966)

40) L. Grodzins et al., Phys. Lett. 24B, 282 (1967)

41) Bickel et al., (to be published)

42) E.M. Burbidge, G.R. Burbidge, W.A. Fowler and F. Hoyle, Rev. Mod. Phys. 29, 547 (1957)

43) L.H. Aller, Astrophysics: Nuclear Transformations, Stellar, Interiors, and Nebulas (Ronald Press, New York, 1954)

44) R.V. Wagoner, W.A. Fowler, and F. Hoyle, Astrophy. J. 148, 3 (1967)

45) C.H. Corliss and W.R. Bozman, Nat. Bur. Standards Monograph 53

46) J.L. Greenstein and M. Schmidt, Astrophy. J. 148, 113 (1967)

47) C.R. Lynds, Beam Foil Spectroscopy (Gordon and Breach, New York, 1968)

48) R. Tousey, Beam Foil Spectroscopy (Gordon and Breach, New York, 1968)

49) W.L. Wiese and A.W. Weiss, Phys. Rev. 175, 50 (1968)

INSTITUTIONS CURRENTLY ACTIVE IN BFS

Aarhus, Univ. of	Aarhus, Denmark
Air Force Cambridge Research Labs	Bedford, Massachussets, US
Alberta, Univ. of	Edmonton, Canada
Arizona, Univ. of	Tucson, Arizona, US
Australian National Univ.	Canberra, ACT, Australia
Calif. Inst. of Technology	Pasadena, California, US
Carnegie Inst. of Washington	Washington, DC, US
Copenhagen, Univ. of	Copenhagen, Denmark
Kansas State Univ.	Manhattan, Kansas, US
Laval Univ.	Quebec, Canada
Lyon, Univ. of	Lyon, France
Murray State Univ.	Murray, Kentucky, US
New Hampshire, Univ. of	Durham, New Hampshire, US
New York Univ.	New York, NY, US
Oak Ridge National Laboratory	Oak Ridge, Tennessee, US
Research Inst. for Physics	Stockholm, Sweden
Rice Univ.	Houston, Texas, US

INSTITUTIONS PREVIOUSLY ACTIVE OR NOW CONTEMPLATING BFS WORK

California, Univ. of	Berkeley, California, US
Los Alamos Scientific Lab	Los Alamos, New Mexico, US
Naval Research Laboratory	Washington, DC, US
Northwestern Univ.	Evanston, Illinois, US
Oregon State Univ.	Corvallis, Oregon, US
Rensselser Polytechnic Inst.	Troy, NY, US
State Univ. of New York	Oyster Bay, NY, US
Texas, Univ. of	Austin, Texas, US
Virginia Polytechnic Inst.	Blacksburg, Virginia, US
Virginia, Univ. of	Charlottesville, Virginia, US
Wisconsin, Univ. of	Madison, Wisconsin, US